



Guest editors:
K. Buchanan and S. Staddon

Taylor & Francis Group
ISSN 0961-3218 (Print) 1466-4321 (Online) Journal homepage: <https://www.tandfonline.com/loi/rbri20>

Routledge
Taylor & Francis Group

ISSN: 0961-3218 (Print) 1466-4321 (Online) Journal homepage: <https://www.tandfonline.com/loi/rbri20>

Challenges in the low-carbon adaptation of China's apartment towers

C. Alan Short, Jiyun Song, Laetitia Mottet, Shuqin Chen, Jindong Wu & Jian Ge

To cite this article: C. Alan Short, Jiyun Song, Laetitia Mottet, Shuqin Chen, Jindong Wu & Jian Ge (2018) Challenges in the low-carbon adaptation of China's apartment towers, Building Research & Information, 46:8, 899-930, DOI: [10.1080/09613218.2018.1489465](https://doi.org/10.1080/09613218.2018.1489465)

To link to this article: <https://doi.org/10.1080/09613218.2018.1489465>



© 2018 The Author(s). Published by Informa UK Limited, trading as Taylor & Francis Group



[View supplementary material](#)



Published online: 11 Jul 2018.



[Submit your article to this journal](#)



Article views: 496



[View Crossmark data](#)



Challenges in the low-carbon adaptation of China's apartment towers

C. Alan Short ^a, Jiyun Song  ^{a,b}, Laetitia Mottet  ^{a,c}, Shuqin Chen^d, Jindong Wu^d and Jian Ge^d

^aDepartment of Architecture, University of Cambridge, Cambridge, UK; ^bDepartment of Applied Mathematics and Theoretical Physics, Centre for Mathematical Sciences, University of Cambridge, Cambridge, UK; ^cApplied Modelling & Computation Group, Department of Earth Science and Engineering, Imperial College London, London, UK; ^dDepartment of Architecture, Zhejiang University, Hangzhou, China

ABSTRACT

Low-carbon building retrofit will contribute to delivering China's policy to reduce carbon emissions. This paper proposes viable low-carbon adaptation strategies for a recurrent building type within the Hot Summer and Cold Winter (HSCW) zone. An existing 23-storey tower in Hangzhou is investigated within the context of a representative city environment. Indoor air temperatures and energy consumption were monitored across a typical floor and simulated in EnergyPlus. Outdoor and indoor airflow patterns were modelled in an advanced computational fluid dynamics (CFD) tool, FLUIDITY. Across a typical floor, observations and modelling show marked variations. South-facing flats overheat significantly in summer largely due to solar radiation. External sun-shading structures are proposed and evaluated to counter summer overheating. An innovative wind catcher and exhaust-stack natural ventilation system is proposed to enhance indoor thermal comfort using natural ventilation. Modelling of this integrated ventilation system indicates that the proposed retrofit system will improve indoor thermal comfort even in the lower floors. The proposed building retrofit strategy is costed using locally established construction cost estimates. Predicted energy savings suggest that the adaptation strategy proposed is potentially viable with significant implications for policy-makers, developers, constructors and designers in this challenging climate zone in China.

KEYWORDS

adaptation; buildings; low carbon; natural ventilation; retrofit; tall buildings; China

Introduction

Excessive energy consumption and carbon dioxide (CO₂) emissions (Wang, Zhou, Zhou, & Wang, 2011; Zhang & Cheng, 2009) have historically accompanied the rapid urbanization of China, as delivered by its buoyant construction industry. In fact, construction industry growth has outstripped growth in China's gross domestic product (GDP) (Luo & Gale, 2000). The building sector is currently responsible for 36–40% of total energy consumption in China (Tsinghua University Building Energy Research Centre (THUBERC), 2016; Zhang, He, Tang, & Wei, 2015). Heating, ventilation and air-conditioning (HVAC) account for 47% of building energy consumption and, therefore, up to 18.8% of overall energy consumption in China (Zhang et al., 2015). In an attempt to reduce emissions, China's central government has set the ambitious target of reducing CO₂ emissions per unit of GDP by 40–45% by 2020 against the

2005 baseline (Ministry of Housing Urban and Rural Development (MOHURD), National Development and Reform Commission (NDRC), 2013). Li and Yao (2012, p. 419) emphasize that 'CO₂ emission cuts will be a major target for China's medium- to long-term economic and social development plans'.

Regional and China-wide green building councils have been launched to encourage the design, construction and renovation of buildings to increase energy efficiency and reduce pollution throughout the whole life cycle (China Urban Research Committee (CURC), 2008; NDRC, 2011; Wang et al., 2011). There is a recognition that existing traditional design processes obstruct the implementation of this policy. More collaborative working is promoted across policy-makers, stakeholders, researchers and professionals to achieve a more integrated approach considering social, economic and environmental impacts (Li & Yao, 2012). The current paper describes such a collaborative process exploring

adaptation potential in the existing building stock in a particular climate zone, spanning Chinese and UK researchers, designers and constructors.

This research is part of a larger study Low Carbon Climate-Responsive Heating and Cooling of Cities (LoHCool) designed to confront the problem of enhancing winter and, more particularly, summer thermal conditions, but with significantly reduced associated carbon emissions. It investigates the retrofit potential of the existing building stock of the cities in the environmentally challenging Hot Summer and Cold Winter (HSCW) zone of China. The whole region is located below the latitude of the Huai River–Qin Mountain axis demarcated by central government to identify the HSCW zone to the south where central heating and, by implication, cooling is proscribed (Figure 1(a)).

LoHCool concentrates on increasing resilience to climate and thereby adding value to the existing urban building stock in this region so that it may be retained, some 9 billion m² of gross internal floor area in 2012, much of it built in the preceding 30 years. The research

is case study based, employing seven case studies, four in Hangzhou, three in Chongqing, that aim to generate practical and viable adaptation design strategies for the representative recurring building types observed in the cities under consideration, Hangzhou (Figure 1(b)) and Chongqing. LoHCool researchers, mindful of air quality concerns, collaborate actively with the UK Engineering and Physical Sciences Research Council's (EPSRC) Grand Challenges project 'Managing Air for Green Inner Cities (MAGIC)' focused on understanding urban air quality.

Liu (2017) reports that in Chongqing between June and August 2016, portable domestic air-conditioning (AC) units, the default means of achieving elementary local environmental control in the zone, operated in cooling mode for 40–60% of the time, a tendency one might track against the three-fold rise in per capita income in Chongqing between 2005 and 2016. However, the AC units were operated in heating mode in winter for only 10% of the time. Demand for mechanical cooling is the key issue in reducing carbon emissions in the HSCW zone. A total of 550 million citizens inhabit the HSCW zone, 53% of whom live in its cities. If the *business-as-usual* solution of sealing and AC buildings is adopted wholesale, a carbon penalty of prodigious proportions will result. Costanzo (2017) reports a decrease in energy intensity in Chongqing by two-thirds from levels before 2001 to 2010, but almost all of this saving is in winter heat energy.

This paper focuses on resolving the adaptation challenges of a representative case study building in Hangzhou city. Hangzhou is identified by Tong, Chen, Malkawi, Liu, and Freeman (2016) as proportionally the most favourable city in China in which to employ natural ventilation. The 23-storey Liubo building, an apartment tower of a demonstrably recurrent type in Hangzhou and beyond, has a configuration quite foreign to Europe and North America: a squarish floor plate with deep re-entrants to connect bathrooms, kitchens and supplementary bedrooms deep within the plan to the external environment.

More detailed information about the Liubo building and the Hangzhou study area is given in the next section. To understand better both the current and the predicted retrofitted building performance, the computational fluid dynamics (CFD) model FLUIDITY (AMCG, 2015) was employed to simulate the turbulent air flows around and inside the buildings within a dense urban context in conjunction with a building energy model (EnergyPlus, 2017) to simulate the indoor thermal condition and energy consumption of both existing and retrofitted scenarios. The methodology behind FLUIDITY and EnergyPlus is presented in the fourth section.

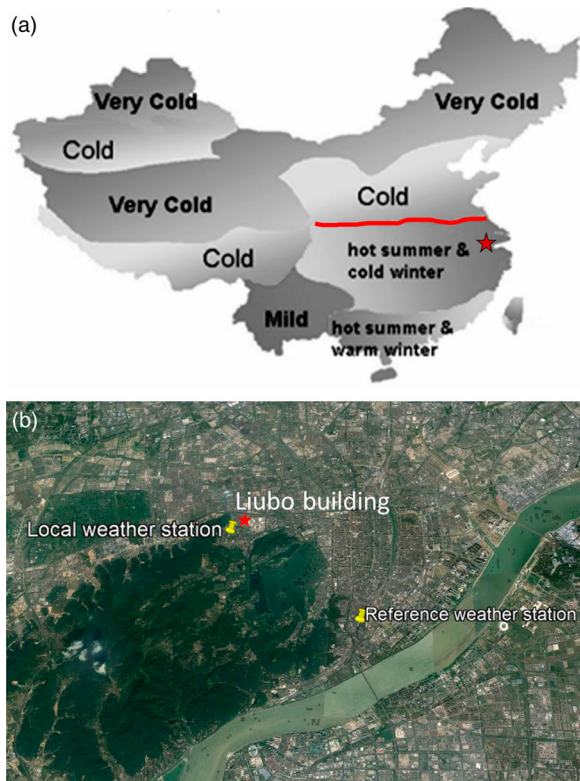


Figure 1. (a) The five climate zones for building thermal design in China and the demarcation (red) line known as the Huai River–Qin Mountain Line, south of which central heating and cooling is not envisaged by current central government policy. Source: Adapted from Li et al. (2014). The city of Hangzhou is depicted by the red star. (b) Aerial view of Hangzhou showing the locations of the Liubo case study building, the local weather station and the reference weather station. Source: Google Maps.

Study area and climate information

Typical building types in the study area

A sample strip within which to explore prevalent building typologies was configured by Zhejiang University researchers (Ge & Yu, 2016) across the Xihu and Xiacheng districts, effectively the centre of Hangzhou, 0.5 km wide by 2 km long, containing 292 buildings, 206 of which were residential with 30 offices and four commercial buildings, 10 hotels, one hospital and 41 educational buildings. The analysis sorted the sample buildings into three categories by floor plate form: point-type buildings presenting facades less than 30 m wide to neighbouring buildings, in effect towers similar to the Liubo building; 'plank-type' buildings presenting facades greater than 30 m wide, in effect 'slabs'; and 'other plate forms' including atria, open-plan and ambulatory types. The plate form types were further sorted by age relating to the incremental improvement in environmental performance required by succeeding Chinese standards denoting four meaningful periods: before 1986, 1986–95, 1995–2003 and after 2003. Orientation, numbers of storeys, construction, structure and cooling/heating strategies were also recorded to yield insights into factors affecting residential electricity consumption. Building area, plate form, height, heating and cooling sources, and date of construction emerged as most significant. The study reveals that 77% of the sample area buildings belong to the point-type (tower) before 1986, 25% in the 1986–95 category and 21% in 1995–2003 so that the 1995 Liubo building spans the latter two categories.

Case study building

The Liubo building is a concrete-framed tower built in 1995, just ahead of the third energy conservation revision to the building regulations. It has floor plates of 508.5 m² gross internal area, encompassing 12,204 m² total floor area across 23 occupied floors. Floor to ceiling heights are a generous 2.7 m. It has no central mechanical ventilation and no provision for central heating or cooling in line with central government policy in the HSCW zone. Ventilation is achieved by opening windows, all of which are of the single-glazed aluminium sliding type, apparently ubiquitous in the region. Figure 2 shows a typical floor plan of eight flats arranged so that each flat has at least two external walls with free access to the external environment. The areas of flats 1–8 are 40.46, 51.82, 54.84, 52.44, 40.46, 51.82, 54.84 and 52.44 m² respectively. All accessible balconies have been subsequently enclosed with sliding glazing. The axis of symmetry is north–south and the

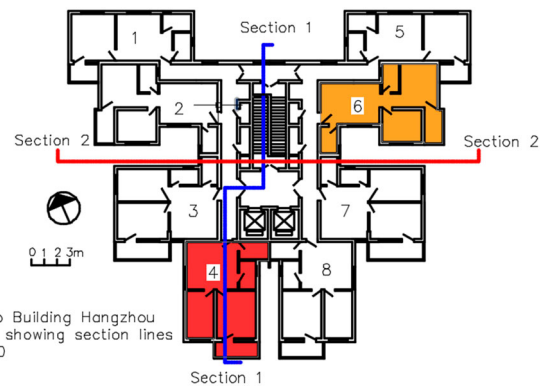


Figure 2. The Liubo building: typical floor plan showing the relative locations of the case study flat 4 on level 5 and flat 6 on level 3. Levels 3 and 5 are identical.

plan splay to give the four flats on the north side some view southwards. A section along the north–south axis is shown in Figure 3(a). Reflecting the southernmost four flats about the east–west axis along which section 2 (Figure 3(b)) is taken would give a highly typical square plan with deep re-entrants to all orientations, common, for example, in Hong Kong. The construction elements are summarized in Table S1 in the supplemental data online.

Figure 3(b) shows that fire safety is reinforced by the ingenious nesting of two staircases within each other, but isolated from each other by three lobbies and four fire-rated doors along both approaches within a compartmented shaft at the core of the building. Flats have steel outer doors and timber inner doors at the threshold to the common corridors. The China and UK researchers propose to leave this arrangement intact and unaltered so that what might appear to offer a substantial and efficient potential ventilation stack at the core of the building, very apparent in Figure 3(b), is not pursued in adaptation proposals in order to maintain safe vertical and horizontal escape routes free of smoke.

Climate information in the study area

Typical weather data across the HSCW zone are available from the Meteorological Information Center of the China Meteorological Administration (CMA) and the Department of Building Technology & Science of Tsinghua University joint publication of 2005 (in Chinese). The published data provide averaged climate data from 1971 to 2003 for the city of Hangzhou from data collected at a reference weather station (30.23N, 120.17E), yielding a typical meteorological year (TMY). These data form the climate database for EnergyPlus

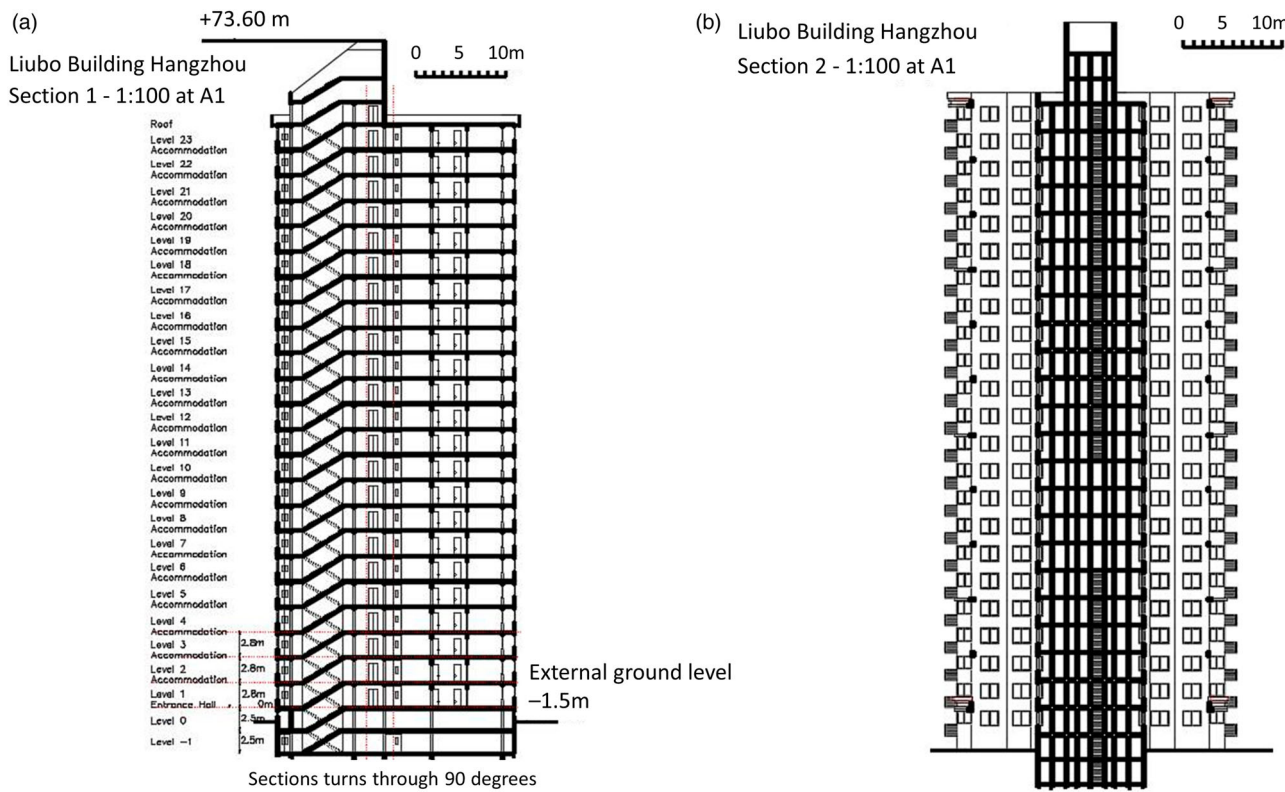


Figure 3. The Liubo building: (a) section 1: north–south looking east; and (b) section 2: east–west looking north. The locations of both sections are indicated on the plan shown in Figure 2.

modelling of buildings within the Hangzhou region. To complement the TMY, weather data were collected by LoHCool colleagues at Zhejiang University from a local weather station located on the roof of a university research building (30.263°N , 120.1175°E) close to the Liubo building (30.2662°N , 120.1260°E) to reveal any local variation. The relative locations of the case study Liubo building, the local weather station and the reference weather station are shown in Figure 1(b). The reference weather station is located close to the Qiantang River, which crosses the locality from north-east to south-west, with hills to the north-west separating the campus from the central West Lake area.

During the summer period (July–August), the mean TMY temperature reaches $28\text{--}29^{\circ}\text{C}$, while during the winter (January) the lower mean temperature is 5°C . August is the hottest month (mean of 29°C) and the most humid (around 20 g/kg humidity ratio). Given the potential cooling energy requirement against contemporary comfort criteria, August is of prime interest to LoHCool.

Figure S1 in the supplemental data online shows the daily variation in air temperature and the relative humidity for August for data from the TMY and the local weather station. August peak temperatures are higher at the case study site, of the order of 4°C , so that

occasional peaks of 35°C in the TMY data have become a series of peaks of 39°C over the 20 days in which data were successfully gathered. According to the Zhejiang Climate Impact Assessment report (Zhejiang Climate Center, 2017), the summer in 2017 was warm with an average temperature of 27.8°C , 0.8°C higher than a normal year. The number of hot days in July–August is recorded as increasing.

As shown in Figure S2 in the supplemental data online, an explanation may be provided in part by comparison of historical solar radiation levels measured through August 12–31, 2001, peaking at 922 W/m^2 , with local weather station data for the same month in 2017 reaching 1148 W/m^2 . Solar radiation intensity appears to be increasing from a TMY August mean of $13.29 \text{ MJ/m}^2/\text{day}$ to $19.44 \text{ MJ/m}^2/\text{day}$.

August wind roses are shown in Figure 4. The reference weather station wind rose for August (Figure 4(a)) shows that easterly winds dominate, achieving speeds up to 6 m/s , while the August data gathered by the local weather station adjacent to the Liubo building (Figure 4(b)) reveal a more variable distribution and lower wind speed. The reference weather station is located close to the Qiantang River (Figure 1(a)), enabling the easterly winds to predominate (Figure 4(a)). The campus lies between two ranges of hills in an

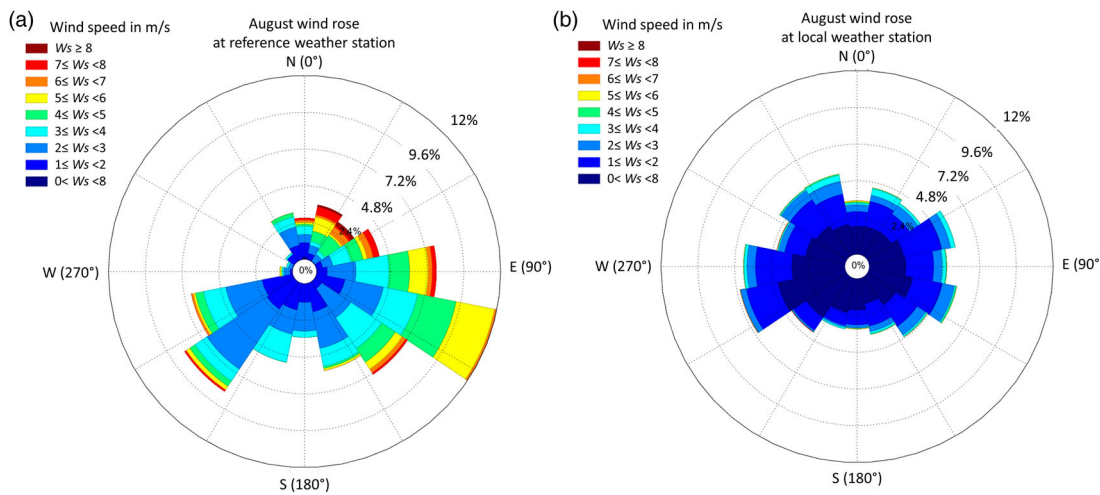


Figure 4. August wind roses generated (a) from the typical meteorological year (TMY) at the reference weather station and (b) from the local weather station.

urban area with dense building arrays (Figure 1(b)), so the wind speed at the local weather station is therefore significantly lower (Figure 4(b)).

Indoor comfort criteria for naturally ventilated buildings in the HSCW zone

Historical and current approaches to predicting indoor thermal comfort in alternately warm and cold continental climates (Song, 2017) are derived from Western standards based on Fanger's (1970) methodology of predicted mean vote (PMV) and percentage people dissatisfied (PPD) embodied in the American Society of Heating, Refrigerating and Air-Conditioning Engineers' (ASHRAE) Standard 55-2004 (ASHRAE, 2004). However, actual surveyed responses differ markedly from those predicted using this method in the HSCW zone, whose residents emerge as being actively and physiologically adaptive (Yao, Li, & Liu, 2009). Li, Yu, Liu, and Li (2011) report significant differences between predicted neutral temperatures (T_n) for the eight cities of the Yangtze River Region: in winter of 20.1°C against an actual measured T_n of 17.5°C and in summer of 26°C against an actual measured T_n of 27.6°C. In fact, Li et al. recorded that the 80% acceptable temperature range for the eight major cities of the HSCW Yangtze River Region in residential buildings was 16.3–28.1°C, confirmed by region-wide surveys between 2007 and 2011 (Li, Yao, Wang, & Pan, 2014). This admits a more pragmatic approach to adaptation and is in line with findings elsewhere informing adaptive thermal comfort theory which envisages occupants as active participants exercising psychological and physiological adaptation in free-running buildings (de Dear & Brager,

1998). LoHCool adopts these criteria in assessing performance in the case study buildings.

Adaptation potential in the built environment

Retrofit and adaptation

Dixon and Eames (2013) reinforce the need for effective links between research, policy-making and practice in 'retrofitting' or re-engineering existing urban environments. A series of papers support their position on regenerative design, re-engineering and retrofitting cities (Cole, 2012; Dawson, 2007; Kelly, 2009). Dixon and Eames (2013) prefer the term 'retrofit' (the concept guiding the UK EPSRC programme 'Retrofit 2050'), while the LoHCool project team employs the term 'adaptation'.

Kelly (2009), former Chief Scientific Officer to the UK Department for Communities and Local Government, concluded:

There are four ways by which the carbon emissions from existing buildings can be tackled: re-engineering the fabric of buildings [...]; improving the efficiency of appliances used in the home; decarbonising the sources of energy to the home [...]; changes in personal behaviour. (p. 198)

LoHCool explores the first strategy primarily, but in its essentially passive design approach exploits the third. The project also looks to enhanced occupant control, but this lies beyond this paper's scope, inviting future work in monitoring the implementation of a similar adaptation scheme.

Understanding the current and likely behaviour of occupants in adaptive retrofits is essential. Li and Yao (2012, p. 428) emphasize 'Research into end-user

behaviour on energy consumption in buildings is required, particularly in residential buildings'. Kelly (2009) records that:

Data from China ... shows that the elderly are economical and the younger are profligate consumers, with a factor of three-to-five difference in intensity of use for an identical headcount! This highlights the important role of psychology by managing expectations and creating acceptable forms of consumer behaviour. (p. 199)

LoHCool was fortunate that Zhejiang University staff living and working in the project case study buildings were prepared to be monitored and keep an account of both their occupancy and their window-opening regime. LoHCool's adaptation schemes deliberately externalize as much of the new infrastructure as possible to limit intrusion into residents' dwellings and avoid the need to evacuate the apartments for a period. Li and Yao (2012) identify the lack of an integrated interdisciplinary approach as a major barrier to successful implementation of effective schemes. LoHCool's collaborative interdisciplinary work method between Chinese and UK researchers is very much oriented to developing such an approach. An important part of the LoHCool agenda is to demonstrate how value can be recovered in existing buildings of the relatively recent past to encourage their retention with considerable savings in embodied energy.

Solutions for building adaptation

Amongst solutions to reduce the energy consumption and CO₂ emissions of buildings within the scope of reengineering the building fabric, designers and clients should consider: the orientation of the building (Aflaki, Mahyuddin, Mahmoud, & Baharum, 2015; Zhou, Wang, Chen, Jiang, & Pei, 2014); the building envelope (Chow, Li, & Darkwa, 2013; Ge, Wu, Chen, & Wu, 2018; Liu, Liu, Ye, & Liu, 2018); its windows (Chow et al., 2013; Liu et al., 2018; Zhou et al., 2014); the replacement of boilers (Chow et al., 2013; Liu et al., 2018); the use of natural ventilation (Aflaki et al., 2015; Liu et al., 2018; Lomas, Giridharan, Short, & Fair, 2012; Zhou et al., 2014); and the use of sun shading (Ge et al., 2018; Short, Lomas, et al., 2012). Two parallel adaptation strategies will be addressed and discussed: the use of advanced natural ventilation (Lomas, 2007) and the installation of external sun shading.

Natural ventilation

Natural ventilation consists of supplying fresh outdoor air into the indoor space. Three main natural ventilation modes are identified: single-sided ventilation, cross-ventilation and stack ventilation (Chenari, Carrilho, & Gameiro Da Silva, 2016). These modes can occur at the

same time, inducing a competition between wind effect and buoyancy forces. The design of natural ventilated buildings is still challenging due to the constant changes in external weather conditions (wind speed and direction, for example) and the impacts of surrounding buildings, explaining why the informed use of CFD models for the design of natural ventilation schemes is so powerful (Asfour & Gadi, 2007; Blocken, 2014; Chen, 2009).

Numerical study of natural ventilation. The efficiency of single-sided natural ventilation of a simple isolated and rectangular building has been thoroughly investigated. The room aspect ratio (Asfour & Gadi, 2007); the height of two opposing openings (Meroney, 2009; Peren, Van Hooff, Leite, & Blocken, 2015a); the roof shape (Peren et al., 2015a; Peren, Van Hooff, Leite, & Blocken, 2015b, 2016); the impact of wing walls (Mak, Niu, Lee, & Chan, 2007); the influence of internal obstacles (Chu & Chiang, 2013); and the numerical model parameters (Ramptoni & Blocken, 2012; Van Hooff, Blocken, & Tominaga, 2017) comprise a non-exhaustive list of parameters numerically studied to highlight their influences on natural ventilation in simple circumstances.

More complex geometry in a single isolated building has also been numerically studied to quantify the efficiency of natural ventilation in more realistic building configurations (Carrilho Da Graca, Chen, Glicksman, & Norford, 2002; Essah, Yao, & Short, 2017; Hajdukiewicz, Geron, & Keane, 2013; Muhsin, Yusoff, Mohamed, & Sapian, 2017; Short, Noakes, Gilkeson, & Fair, 2014; Tong, Chen, Malkawi, Adamkiewicz, & Spengler, 2016; Wang & Wong, 2008; Wu, Yang, Tseng, & Liu, 2011; Yang, Wen, Juan, Su, & Wu, 2014).

The majority of numerical studies of natural ventilation have focused on an isolated building rather than on building groups. This is surprising given the impact of surrounding buildings. Indeed, the accuracy of natural ventilation potential is strongly dependent on the *influence region* chosen around the case study building. Few studies highlight the impact of the surrounding buildings on the predicted ventilation performance of a rectangular building (Cheung & Liu, 2011; Jiang & Chen, 2002; King et al., 2017; Ramponi, Blocken, De Coo, & Janssen, 2015; Tong, Chen, & Malkawi, 2016). In the previously cited works, the arrangement of surrounding buildings is well organized in simple configurations with regular or staggered alignments.

Less common applied studies of specific naturally ventilated buildings within their surroundings can be found in the literature: a stadium in the Netherlands (Van Hooff & Blocken, 2010); a university (Mochida, Yoshino, Takeda, Kakegawa, & Miyauchi, 2005) and a residential (Jiang & Chen, 2002) building in Japan; and

a dairy cattle building in Denmark (Wu, Zhai, Zhang, & Nielsen, 2012).

Numerical models. Various researchers have proposed to couple building energy simulation with CFD to assist architects in the design of naturally ventilated buildings (Guo, Liu, & Yuan, 2015; Omrani, Garcia-Hansen, Capra, & Drogemuller, 2017). Guo et al. (2015) describe a methodology to optimize the building's natural ventilation using CFD simulation based on site planning, building shape and the building envelope. Six design steps were identified by Omrani et al. (2017) who suggested that CFD simulations are a useful tool to inform concept and subsequent detailed design.

The majority of CFD studies of natural ventilation have been conducted with the steady Reynolds-averaged Navier–Stokes (RANS) approach. Some exceptions are the studies by Jiang and Chen (2002), Meroney (2009) and Chu and Chiang (2013), who used large eddy simulations (LES). From a fluid dynamics point of view, it has been shown that the RANS approach is not appropriate to model highly turbulent flows such as those occurring in complex urban environments and natural ventilation processes, suggesting that using the LES approach to estimate natural ventilation efficiency is more appropriate (Ramponi et al., 2015; Salim, Ong, & Cheah, 2011; Van Hooff et al., 2017). In fact, the RANS approach does not convincingly capture the unsteady fluctuation term of turbulence which is crucial to describe fully the flows, the turbulent mixing process and the transport of pollution.

Features intended to enhance natural ventilation. The enhanced effectiveness of natural ventilation using various features to promote flows such as atria, wind towers, wind catchers and ventilation stacks has been demonstrated (Chenari et al., 2016; Khan, Su, & Riffat, 2008). The plan form of the residential Liubo building does not enable the use of an atrium but will accommodate ventilation stacks and wind catchers.

A ventilation shaft (or chimney) consists of a vertical space used to create a passage for encouraging vertical air circulation (Chiu & Etheridge, 2007; Lomas, 2007; Prajongsan & Sharples, 2012; Priyadarsini, Cheong, & Wong, 2004; Short, Lomas, et al., 2012; Short, Yao, Luo, & Li, 2012; Yang et al., 2014). The stack can be active (with a fan at the top, for example) or passive (Priyadarsini et al., 2004) for buildings where only single-sided ventilation could otherwise be performed. Judiciously applied, this system permits the occupant to be more comfortable during warm summer conditions (Prajongsan & Sharples, 2012; Yang et al., 2014), reducing AC energy consumption (Prajongsan & Sharples, 2012). The efficiency of the stack

is affected by the area of the openings (Priyadarsini et al., 2004) and the height of the stack (Lomas, 2007). A promising stack ventilated hybrid scheme in Beijing is reported by Essah et al. (2017) in which mechanical heating and cooling is employed for half the year, the mid-seasons being free running, saving some 50% of energy consumption.

The terminations of both passive and active ventilation stacks play an essential role in their effectiveness in dissipating exhaust air into the atmosphere while preventing downdraughting of the air (Khan et al., 2008). Carpenter (1990) studied eight anti-downdraught chimney terminations under different wind angles and positively identified the H-Pot (refers to the termination outputs with two offset outputs to form the outline of the letter H) as the most effective termination type. The effectiveness of this termination type has been understood since the 19th century (Hall, 1880), as demonstrated in retrofitted projects (Short, Lomas, et al., 2012). Su, Riffat, Lin, and Khan (2008) present a monodraught-type alternative termination: a quadripartite louvered development of the traditional wind catcher found in Dubai (UAE) and Yazd (Iran). These terminations encourage flows in and out through opposing cells in exchange flows. Swiegers (2015) offers an effective alternative: the wind-propelled revolving 'whirlybird' exhaust cowl appropriate for smaller scale applications.

The wind tower provides natural ventilation by taking advantage of the pressure differences surrounding the building (Hughes, Calautit, & Ghani, 2012). A Venturi-shaped roof may be used to create a constriction driving partial or total natural ventilation of the building if the wind direction is constant (Van Hooff, Blocken, Aanen, & Bronsema, 2011, 2012). Venturi roof shapes and wind towers are a variant of the wind-catcher tower.

Wind catchers (Jomehzadeh et al., 2017; Saadatian, Chin, Sopian, & Sulaiman, 2012) may be used to increase ventilation rates in exchange flow. These systems, typically located at roof level, have been shown to be efficient in channelling fresh air down into a room. CFD simulations of such configurations have been performed by several research teams (Li & Mak, 2007; Montazeri & Montazeri, 2018; Nejat et al., 2016) in a simple context. Wind-catcher types include: single-side opening (Montazeri & Montazeri, 2018), two side openings (Montazeri & Montazeri, 2018; Nejat et al., 2016) or multiple openings (Li & Mak, 2007; Montazeri, 2011). The two main geometries encountered in the literature are rectangular (Li & Mak, 2007) and circular (Montazeri, 2011) in plan. 'Blades' (Swiegers, 2015; Van Hooff et al., 2011) or wing walls (Nejat et al., 2016) have been employed in an attempt to guide the wind, but unexpected and counterintuitive behaviours can occur (Van Hooff

et al., 2011). Adding guiding vanes increases the flow resistance and causes more wind to flow over and around the system so that less wind enters the target space, in effect obstructing the desired air flow (Blocken, Van Hooff, Aanen, & Bronsema, 2011).

Sun-shading systems

The optimization of natural ventilation intended to cool the indoor environment can be enhanced by reducing the absorption of external heat, notably solar gain. Effective measures include the installation of passive solar shading elements. Shading systems can be divided into two categories: fixed and movable (manual or automated) shading devices (Kirimitat, Koyunbaba, Chatzikonstantinou, & Sariyildiz, 2016). Fixed horizontal sun shading will obstruct daylight in winter, reducing internal light levels (Mandalaki, Zervas, Tsoutsos, & Vazakas, 2012) and remove beneficial light during the winter (Ge et al., 2018). A design compromise has to be achieved (Short, Cook, Cropper, & Al-Maiyah, 2010). Movable shading systems attempt to avoid these drawbacks, but at a cost and with unwelcome complexity. Fixed sun shades (overhangs, horizontal or vertical louvres, egg crates) are usually located externally to the facade, while movable sun shades (venetian blinds, vertical blinds, roller shades) are usually behind the glazing so that solar radiation enters the space. EnergyPlus software is commonly used to study the impact of sun-shading devices on energy consumption and indoor thermal comfort (Kirimitat et al., 2016).

More sophisticated designs for sun shading can be encountered in the literature. Ho, Chiang, Chou, Chang, and Lee (2008) proposed three original fixed designs combining indoor and outdoor elements. Short et al. (2010) proposed a new canted and deep window type, while Short, Renganathan, and Lomas (2015) presented an external sun-shading system composed of diagonal wings designed to maximize the view to the upper sky.

Precedents for adaptation schemes

This section summarizes larger-scale retrofit projects in more temperate climates: in humid, hot summer areas and in the HSCW zone in China.

The project 'Design and Delivery of Robust Hospitals in a Changing Climate' (DeDeRHECC; EPSRC reference number EP/G061327/1) focused on understanding the current performance of hospital buildings in hot summers in the UK, diagnosing the likely causes of overheating against the adaptive comfort criteria for health buildings. The project then developed adaptation proposals out of this diagnostic analysis for a range of types from low-rise buildings to a tower on a podium in a

warming temperate climate (Giridharana, Lomas, Short, & Fair, 2013; Lomas, Giridharan, Short, & Fair, 2012; Short, 2017; Short et al., 2010, 2014, 2015; Short, Lomas, et al., 2012). Subsequently the lead author had the opportunity to implement an adaptation scheme in the context of a continental climate in Beijing (Short, Yao, et al., 2012). The recurrent green elements proposed in the papers cited above include the use of natural ventilation, stacks with various termination and atria, combined with sun-shading systems.

Prajongsan and Sharples (2012) analyzed the potential use of ventilation shafts in tall residential buildings in Bangkok, Thailand, to enhance natural ventilation and improve thermal comfort (and thereby reduce AC energy consumption). By employing the proposed design, the residents are comfortable in their dwelling 56% of the time during the four summer months, against 34% in the current situation.

Chow et al. (2013) proposed a retrofit solution to reduce energy consumption of an existing office building in Ningbo (150 km north-east of Hangzhou) located in the HSCW zone. They proposed renovating the building by changing the enclosure (walls, windows and roof) and replacing the electric boiler with an air-source heat pump. The project cost RMB176.3/m² (US\$26.98/m²) and it provides a reduction of annual energy consumption of 31.24%.

Zhou et al. (2014) presented a design strategy based on CFD modelling for optimizing natural ventilation in high-rise residential buildings in Chongqing, a city in the HSCW zone often viewed as unfavourable for natural ventilation due to low wind speed and pollution. In fact, Tong, Chen, Malkawi, Liu, & Freeman (2016) declared that Chongqing is the city least favourable for natural ventilation amongst 35 cities in China. The adaptation design strategy for new builds included optimizing building orientation, configuring the site layout to create wind paths, and encouraging cross-ventilation by ensuring two opening windows were present in each bedroom, all measures which demonstrate that natural ventilation could be effective in the Greater Chongqing area.

Zha, Zhang, and Qin (2017) showed that solar chimneys can be used for saving energy in residential buildings in Shanghai, also located in the HSCW zone, achieving energy savings of approximately 14.5% during the transitional seasons.

Liu et al. (2018) proposed a retrofit of an 18-storey building located in Beijing. Amongst other measures, they presented a viable system to introduce fresh air into indoor spaces at an additional cost of US\$35.08/m². The air inlets are located along the external walls next to the windows and the waste air is removed at ceiling level. The building envelope, roof and windows are also modified.

Ge et al. (2018) studied the prospects for retrofitting a typical research building located in Hangzhou at the Zhejiang University old campus to reduce energy consumption, particularly the impact of improving the performance of the building envelope and shielding glazing from solar radiation. The sun-shading components proposed, external vertical slats, contribute significantly to the reduction of cooling energy consumption in summer but, in Ge's words, 'make little sense in winter'. Ideally they are dynamic elements that can be folded out of the envelope of winter midday solar radiation.

Methods

Numerical methods

In this section, EnergyPlus version 8.8 is used to simulate indoor thermal conditions and building energy consumption for the case study Liubo building. The geometrical model representation of the eight flats comprising one storey of the Liubo building is shown in Figure 5.

The EnergyPlus model employed the building information data including building construction and building material specifications and thickness given in Table S1 in the supplemental data online, with the weather data given above.

Modelling the effect of increasing ventilation rates on indoor air temperatures and energy consumption commenced by exploring the flow regimes around the Liubo building in the current situation. The flow patterns and pressure distribution around the building were then investigated by CFD simulations performed with FLUIDITY, an open-source finite-element software. For the details of the equations solved and their implementation, see

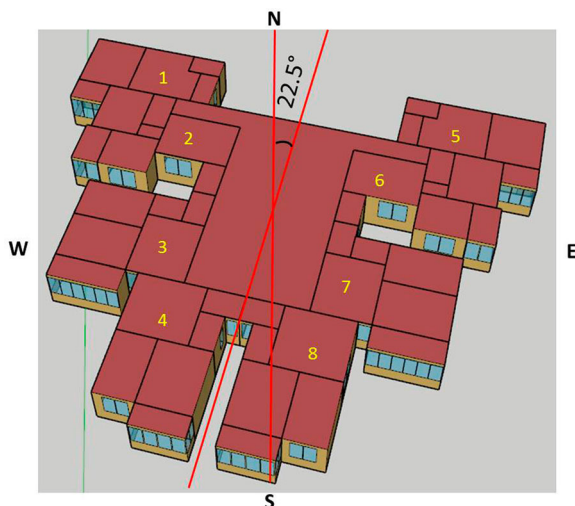


Figure 5. Geometry of a typical floor of the Liubo building as represented in the EnergyPlus model, oriented 22.5° west of south.

Aristodemou et al. (2018), Aristodemou, Bentham, Pain, and Robins (2009), Ford et al. (2004) and Bentham (2003). This model was rigorously validated against analytical solutions (Debay, 2017; Hesse, 2017), wind tunnel experiments (Aristodemou et al., 2009, 2018; Song et al., 2018) and field experiments (Pavlidis, 2011) for estimating indoor natural ventilation as well as outdoor flow regimes. Therefore, for this research task, FLUIDITY is assumed to be an appropriate analytical tool.

Insofar as the external air flows around a building are dependent on the surroundings, the landscape of the surrounding buildings is modelled. As shown in Figure S3 (a) in the supplemental data online, the computational domain represents an area of 95 buildings within Zhejiang University in Hangzhou, including the Liubo building. In order to solve the partial differential equations that govern fluid flow and heat transfer, the domain is split into smaller sub-domains. The governing equations are then discretized and solved inside each sub-domain. The sub-domains are often called elements or cells, and the collection of all elements or cells is called a mesh or grid. The initial mesh used in the simulations is shown in Figure S3(b) online.

The strength of FLUIDITY as an analytical tool is the use of an unstructured and anisotropic adaptive mesh allowing a large number of fine elements in the regions where the physical processes are important, while the mesh is coarser in the regions of less interest (Pain, Umpleby, De Oliveira, & Goddard, 2001). During the simulations, the mesh is characterized by a maximal number of nodes of 6×10^5 and a minimum edge length of elements of 10 cm. To represent the behaviour of the atmospheric boundary layer accurately, a turbulent inlet velocity is prescribed as a boundary condition of the domain. The turbulent inlet velocity is based on the synthetic eddy method (Pavlidis, Gorman, Gomes, Pain, & ApSimon, 2010) and the mean velocity is assumed to follow a log profile. The parameters defining the log-profile law are chosen in accordance with the wind roses presented in Figure 6 to represent typical wind speed during the summer period (August). The turbulence is solved using an LES approach. For more details about the numerical parameters and methods used, see AMCG (2015) and Song et al. (2018). Four different wind directions were simulated: northerly, easterly, southerly and westerly.

Model evaluation

Data in representative flats were collected to inform the calibration of an EnergyPlus model of a typical floor to investigate current and potential performance.

Flat 6 on level 3 (*i.e.* flat 306) was continuously monitored from winter to the hot summer period of August

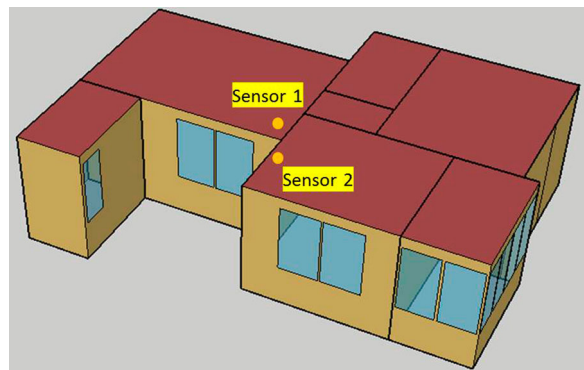


Figure 6. Location of temperature sensors in the test flat (flat 6 in Figure 7) with sensor 1 in the living room and sensor 2 in the bedroom.

2017. The occupants of flat 306 reported that opening the windows at night in midsummer was not effective because external night-time temperatures remain high. Blinds were habitually used behind the balcony glazing. The glazing comprises two sliding panes to the southwest, rarely opened beyond 10 cm, and four to the south-east, one of which tended to be open fully in warm and hot weather. The living room and master's bedroom windows to the south-west tend to be slid

open only to 10 cm. The residents of flat 306 very helpfully permitted colleagues at Zhejiang University to collect data in their absence through two free-running weeks in January (from January 24, 00:00 hours, to January 30, 2017, 00:00 hours) and in August (from August 12, 00:00 hours, to August 18, 2017, 00:00 hours). As a result, there was no electricity usage and no internal heat gains derived from occupancy inside the flat. All exterior windows remained closed with blinds drawn for privacy and security and all interior doors were left open. Figure 6 shows the geometry of the flat and the location of sensors.

Two weeks' of weather data, including air temperature, relative humidity, solar radiation, wind speed and wind direction, were collected from the local weather station and used to drive the EnergyPlus model. Comparison of simulation results against measured indoor air temperatures in the living room and bedroom are presented in Figure 7. The diurnal variations of measured and simulated indoor air temperature are small in both winter and summer, with about a 2°C difference at the widest divergence, implying that the Liubo building can maintain stable temperatures if little or no internal heat gains are present. The root mean square errors (RMSEs) of

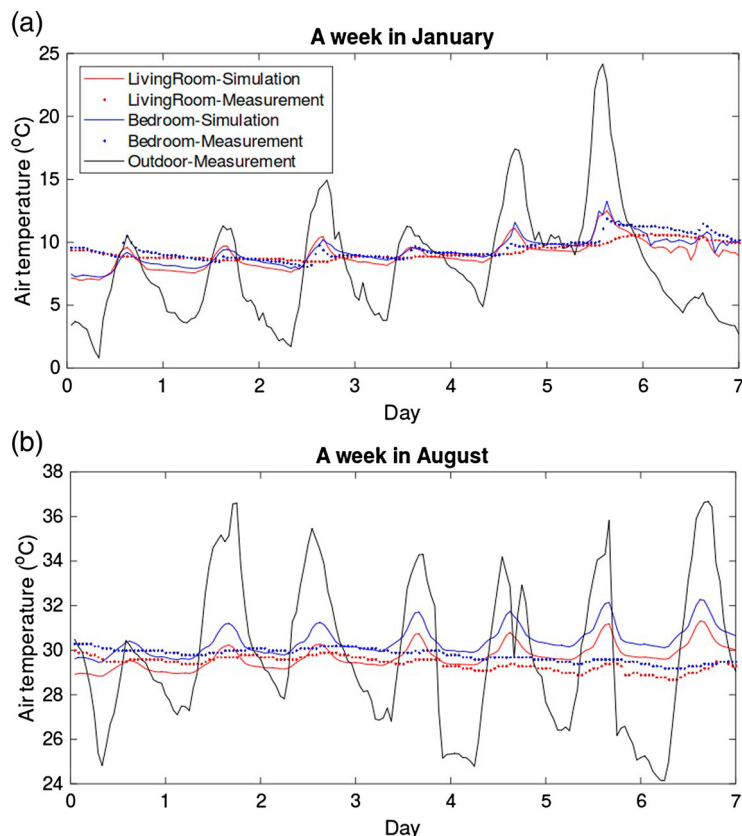


Figure 7. Comparison of model simulations and measurements of indoor air temperatures in both the living room and bedroom of flat 6 when the occupants were absent throughout the week. The flat was free-running, unventilated with all windows closed and blinds drawn for (a) one week in January and (b) one week in August.

simulated and measured indoor temperatures are 1.0 and 0.7°C for the living room in January and August respectively, and 0.8 and 1.0°C for the bedroom in January and August respectively. The current model appears to predict indoor air temperatures with reasonable accuracy. The small variation between simulated and measured indoor temperatures might be a result of differing representative locations. Actual measurements were taken from sensors at the perimeter of each room, while the model outputs the spatially averaged air temperature for each room. Flat 6 is resilient when unoccupied; the challenge is to recover this performance and improve upon it under occupation.

Performance predictions for the existing building condition

After model evaluation and calibration, the EnergyPlus model was run for all eight flats throughout the TMY year. The model assumes casual internal heat gains of 16.7 W/m² deriving from: artificial lighting; occupancy at the rate of one occupant per 17 m² of the floor area; electrical equipment, typically one fridge freezer, one microwave, one bread maker, one television, one laptop, one washing machine and one rice steamer. The variation in indoor temperature in each flat is shown in Figure 8 for January and August. Internal temperatures vary significantly across the eight flats as the solar exposure of the various glazed-in spaces varies by orientation. Figure 8 shows that flats 1 and 5 have the lowest internal temperature whilst flat 4 has the highest internal temperature in both winter and summer. Correspondingly, the heating and cooling energy consumption were calculated on the application of local thermal comfort criteria (16.3–28.1°C) (Li et al., 2011). Figure 9 shows flats 1 and 5 require the highest heating load in winter, while flat 4 requires the highest cooling load in summer to ensure thermal comfort against these criteria. Orientation is found to be a significant factor in influencing the indoor thermal condition and energy consumption. In addition, the simulations show that there exist appreciable mid-season periods (such as April, May, October and November) in which the building can achieve indoor thermal comfort with minimal heating/cooling load, which highlights the practicability of natural ventilative cooling.

Predicted performance of retrofitted adaptation measures

Diagnosis of the observed and predicted performance of selected flats in their existing condition reveals a strong tendency to overheat in the four summer months of

June–September: external dry bulb temperatures periodically approach 40°C whilst night-time temperatures regularly fall to 25–27°C, which is within the regional adaptive comfort band but nonetheless warm for comfortable sleep (Short, Lomas, et al., 2012). The researchers speculated that direct solar gains through the prodigious glazing to balconies contribute materially to the uplift of internal temperatures above peak external such that effective shading would comprise a key element of an adaptation strategy. However, there are appreciable mid-season periods in which little or no energy input is required to maintain comfort: April, May, June and October, November, suggesting appreciable savings are available. Judiciously timed advanced natural ventilation, *i.e.* more controlled and effective than simple opening windows, exploiting the diurnal lows may comprise a second tactic (Lomas, 2007). It may be that peak internal temperatures are lowered by this combined strategy so that cooling demand is much reduced but insufficiently so that some mechanical cooling may still be required, but how does one introduce cooling centrally in the least energy consuming way? Eliminating fan power would be a first step.

Potential effects of external shading on indoor temperatures

Full shading through the summer period will reduce temperature and energy peaks, but the shading structure should admit the maximum available direct sunlight in mid-winter. Figure S4 in the supplemental data online shows a more detailed analysis of the solar geometry at the extensive glazing to flat 4, demonstrably the hottest flat, through the year. Solar altitude is given projected onto the normal to the glazing so that on June 21 at 09:45 hours the angle of incidence in true section is 66.3°, at noon is 83.0° and at 14:30 hours is 82.8°, such that a proportion of the incoming radiation will be reflected back, but the projected angle of incidence falls rapidly thereafter to 32.0° at 16:30 hours. The maximum solar radiation at noon for June is recorded as 1011 W/m². On March/September 21, the projected angle of incidence at 09:45 hours is 55.3°, at noon is 61.9°, at 14:15 hours it remains at 58.0°, falling to 20.3° by 16:30 hours as the sun attacks the west-facing balconies full on. On December 21, however, at noon the projected angle of incidence is 39.2°, by 14:15 hours still at 32.5° but by 16:30 hours it falls to 6.5°C. The maximum solar radiation at noon for December 21 is 594 W/m².

The potential shading effect is simulated using the EnergyPlus model. Figure 10 presents predicted internal temperatures in flat 4 with shading to exclude incrementally 50% and 100% of direct solar radiation. Peak temperatures of 41.4°C are reduced to 39.6°C by halving the

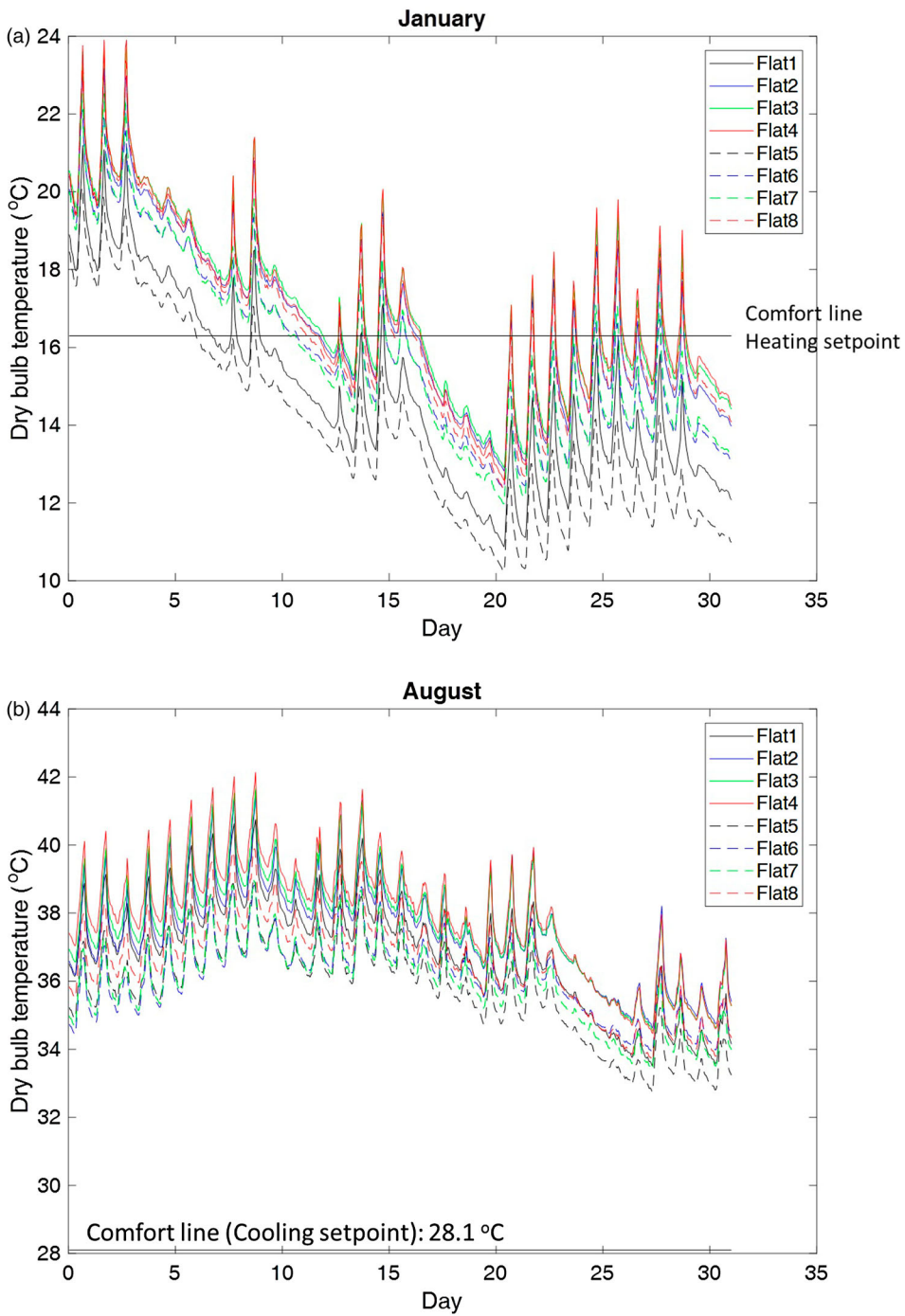


Figure 8. Dry bulb temperature in flats 1–8 as built (EnergyPlus simulation results) for theoretical unoccupied, unventilated free-running periods in (a) January and (b) August.

solar transmittance, and to 37.6°C by wholly excluding direct solar radiation.

Potential effects of enhanced ventilation on indoor thermal conditions

The use of natural ventilation can reduce the energy use of buildings while maintaining a healthy indoor environment. Achieving these two goals can be challenging in a polluted urban environment. Tong, Chen, Malkawi, Liu,

& Freeman (2016) highlight that Hangzhou has the fifth highest energy and CO₂ saving potential through natural ventilation. Tong et al. evaluate the regional feasibility of natural ventilation at the macro-scale and do not include local effects such as building type, shape, local wind pattern and urban geometry or natural ventilation strategies. In order to understand how pollutants concentrate around the Liubo building and to assess the potential use of natural ventilation, CFD simulations were performed.

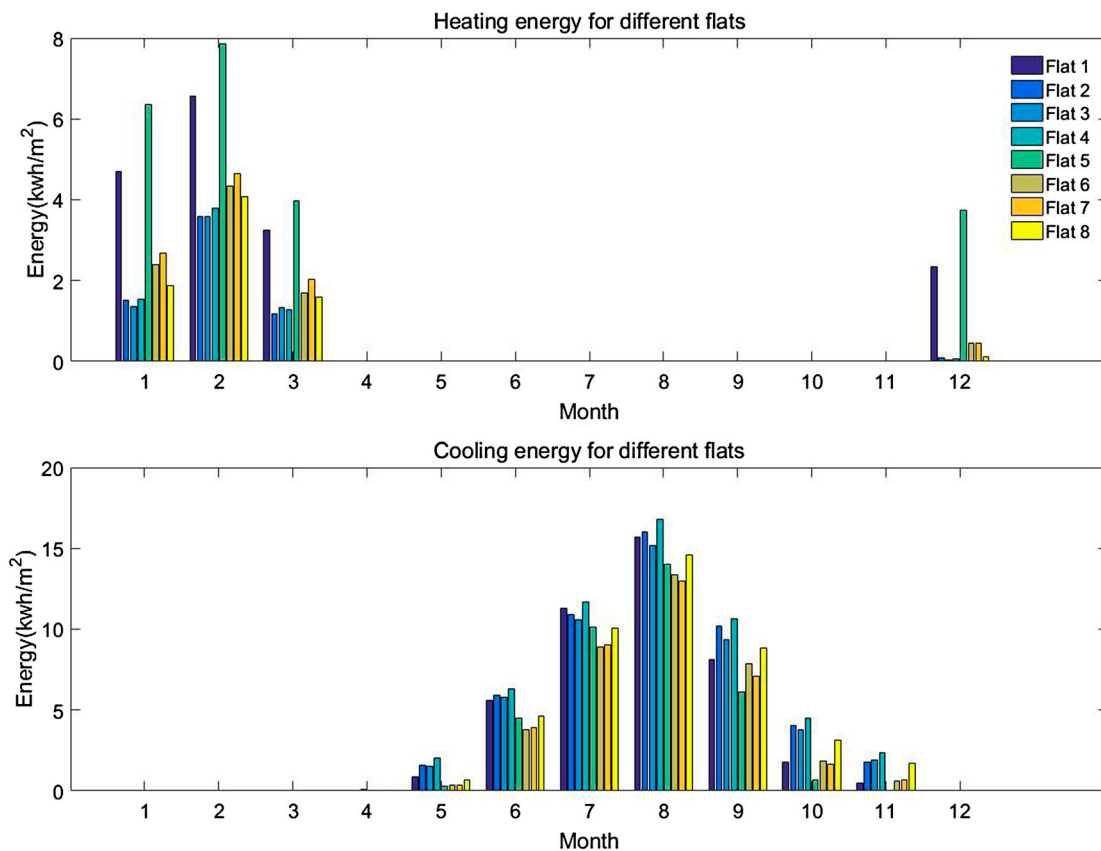


Figure 9. Predicted heating and cooling energy consumption of the eight flats with air-conditioning running as required to maintain thermal comfort within the advised range 16.3–28.1°C. The eight columns in different colours denote flats 1–8 from left to right.

As shown in Figure S3 in the supplemental data online, the geometry includes the surroundings of the building and four main sources of pollution, corresponding to

the four crossroad entry points at which vehicles stop and start (see Figure S3(a) online). Crossroad entry point 2 is more likely to affect the indoor air quality of

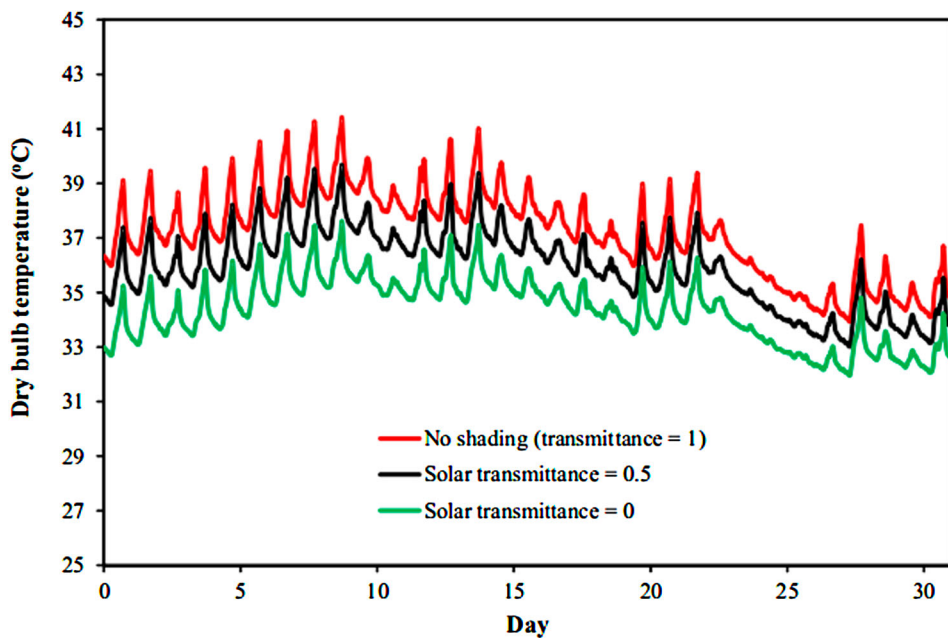


Figure 10. Predicted reductions in mean internal temperatures averaged across the spaces in flat 4 through the year, achieved by effective shading excluding 50% and 100% of direct solar radiation with nil ventilation as predicted by EnergyPlus.

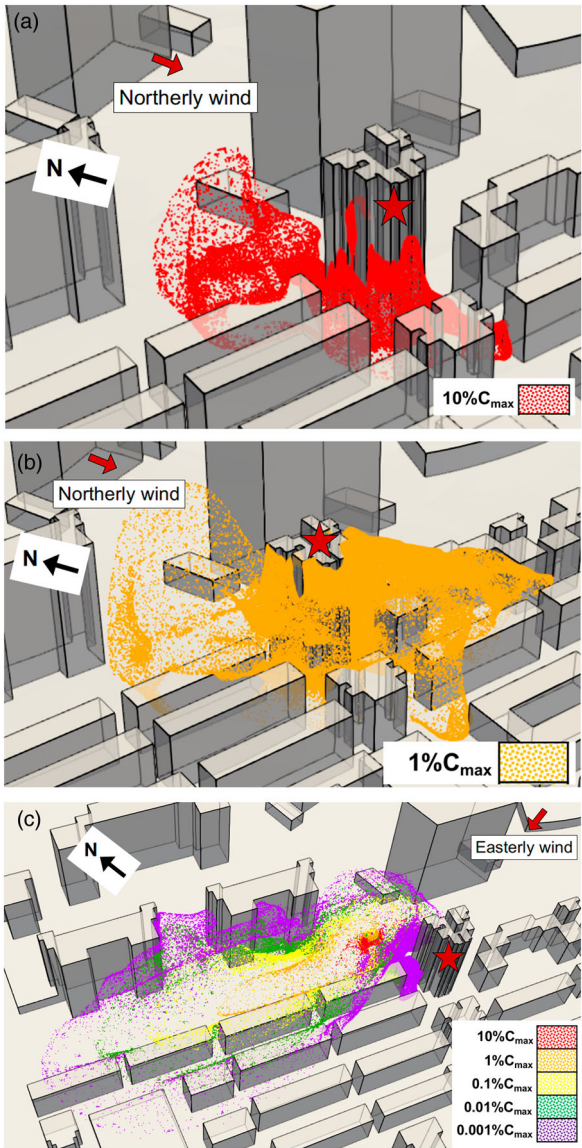


Figure 11. Spread of a pollution source located in the middle of crossroad 2 (Figure 8) located on the north side of the Liubo building for (a, b) a northerly wind and (c) an easterly wind. C_{\max} is the maximum concentration of the pollutant located at the source point. Red stars show the location of the Liubo building. The black arrow denotes north; the red arrows denote the wind direction.

the building and, therefore, the release of a pollutant source (1 kg/s) is numerically simulated in that location. Figure 11 shows iso-surfaces (surface representing points of a constant value) of the pollution for northerly and easterly winds. The maximum concentration C_{\max} is located at the point source in the middle of the crossroad. For a northerly wind, the pollution is mainly trapped on the lower part of the western facade of the Liubo building with a C_{\max} of 10% (Figure 11(a)), while the whole western and southern facades are surrounding by C_{\max} 's of 1% (Figure 11(b)). For an easterly wind, the pollution

is channelled along the street towards the west (Figure 11(c)). For a southerly wind (not shown), the pollutant will be evacuated towards the north of the domain and it does not significantly affect the air quality of the building. The northern facade seems to be less affected by a high level of source pollution.

Figure 12 represents the time-averaged wind speed on a slice at 10 m from the ground for four wind directions: northerly, easterly, southerly and westerly. A blue colour means that the velocity magnitude is equal to 0 m/s, while a red colour represents a high-velocity magnitude (with a maximum of 4.5 m/s). Tall buildings within the domain significantly affect airflow across the campus, strengthening and accelerating flow. The Liubo building has an array of tall buildings to the north disrupting winter northerly winds and a tower immediately to the south. Air is channelled and accelerated between them under frequent easterly and infrequent westerly winds (Figure 12). There are clear opportunities for capturing wind-driven ventilation air and diverting it into the building to increase ventilation rates. To support this idea, the likely flow patterns around the Liubo building as a function of the wind direction are discussed below.

Figure 13 shows the time-averaged velocity vectors around the Liubo building for the four wind directions. The air flow is influenced by the surroundings so that the velocity vectors around the building do not necessarily follow the main wind direction, inducing air-recirculation zones. Three recurrent flow patterns can be identified around the building: a high wind speed zone at the top, created by the extension of the staircase on the roof; air-recirculation zones and zones where the flow follows the shape of the building. The higher wind speeds surrounding the building are located at roof height with the maximum wind speed of 2.6, 3.3, 3.9 and 4.01 m/s respectively for northerly, easterly, southerly and westerly winds. For a northerly wind, the wind speed around the building is at its lowest, with values below 1.5 m/s, whilst reaching values of 3 m/s for the other wind directions. The case study flat is located low down the building on the third floor (*i.e.* 7.4 m from the ground), the most testing location for wind-induced ventilation. The maximum wind speed near case study flat 6 is 0.5 m/s for northerly and easterly winds and 1 m/s for southerly and westerly winds.

As clearly shown in Figure 13, the air-recirculation zones are velocity deficit zones (low wind speed), while the wind tends to be accelerated for flows following the facades. The recirculation zones affect the wind distribution along the facades creating non-uniform flow patterns as a function of height. For example, the higher half of the northern facade is surrounded by a velocity deficit zone (wind speed lower than 0.5 m/s) for southerly

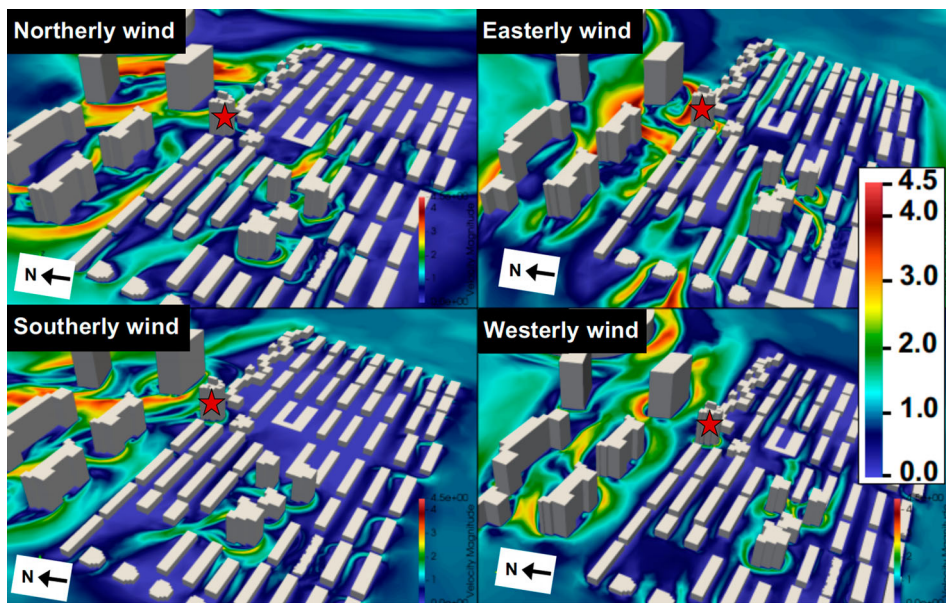


Figure 12. Time-averaged wind speed (m/s) at a horizontal slice at 10 m from the ground for winds blowing from the north, east, south and west. A blue colour means that the averaged velocity magnitude = 0 m/s, while a red colour represents high velocity magnitude (with a maximum = 4.5 m/s). Red stars show the location of the Liubo building.

(Figure 13(c)) and westerly winds (Figure 13(d)). Figure 14 summarizes the main air-recirculation zones around the Liubo building. The eastern facade is exposed to air recirculation for northerly or westerly winds with maximum wind speeds of 1 and 1.5 m/s respectively, whilst air recirculation exists near the western facade for an easterly wind only with maximum wind speeds of 1 m/s. Indeed, for easterly or southerly winds, the air flows follow the shapes of the eastern facade, whereas for northerly, southerly or westerly winds, the air flows follow the geometry of the western facade. Finally, the northern facade is always exposed to air recirculation, except under an easterly wind, while the southern facade is never exposed to air recirculation whatever the wind direction.

The numerical simulations can also provide the distribution of the time-averaged relative pressure on the envelope of the Liubo building. Figure 15 maps the relative pressure distribution for the four wind directions, highlighting that the pressure increases with height. Based on the pressure field obtained numerically, the wind pressure coefficient distribution can be determined on each facade element (Figure 20). The windward facades exhibit higher pressure and wind pressure coefficients than the leeward facade. However, the pressure and subsequently the wind pressure coefficient of the windward facade change slightly for the levels lower than the 10th floor (Figures 15 and 16). Indeed, the lower half of the building is shaded by the surrounding buildings. Above, the absolute value of the pressure coefficients increases markedly with height for floors

higher than the 10th floor (Figure 16). As shown in Figure 16(a), for a northerly wind the pressure coefficient is almost always negative and small (values between 0 and -0.12). This phenomenon is explained by the presence of the tall buildings located on the north side of the Liubo building.

Table 1 summarizes the wind pressure coefficients near the windows of flats 5 and 6 located on the third floor and estimates the maximum flow rate through a fully opened window for wind coming from four different wind angles. A rough approximation of the maximum wind-driven ventilation flow rate (Q_{\max}) across windows can be calculated using (Schulze & Eicker, 2013):

$$Q = C_d \frac{A_{\text{eff}}}{\sqrt{2}} \sqrt{\Delta C_p u}, \quad (1)$$

where C_d is the discharge coefficient equal to 0.65; A_{eff} is the effective opening area (1.35 m^2); and C_p and u are the wind pressure coefficient and velocity (m/s) respectively computed from CFD simulations.

Table 1 clearly highlights that conventional natural ventilation hardly achieves appropriate flow rates, especially for northerly and easterly winds, with values lower than $0.1 \text{ m}^3/\text{s}$, so that airflow in and out of open windows would be very low. Simply relying on opening windows is not an effective strategy.

Figure 17 presents modelled indoor temperatures in flat 306 under various ventilation regimes (no shading) delivering respectively: four air changes per hour

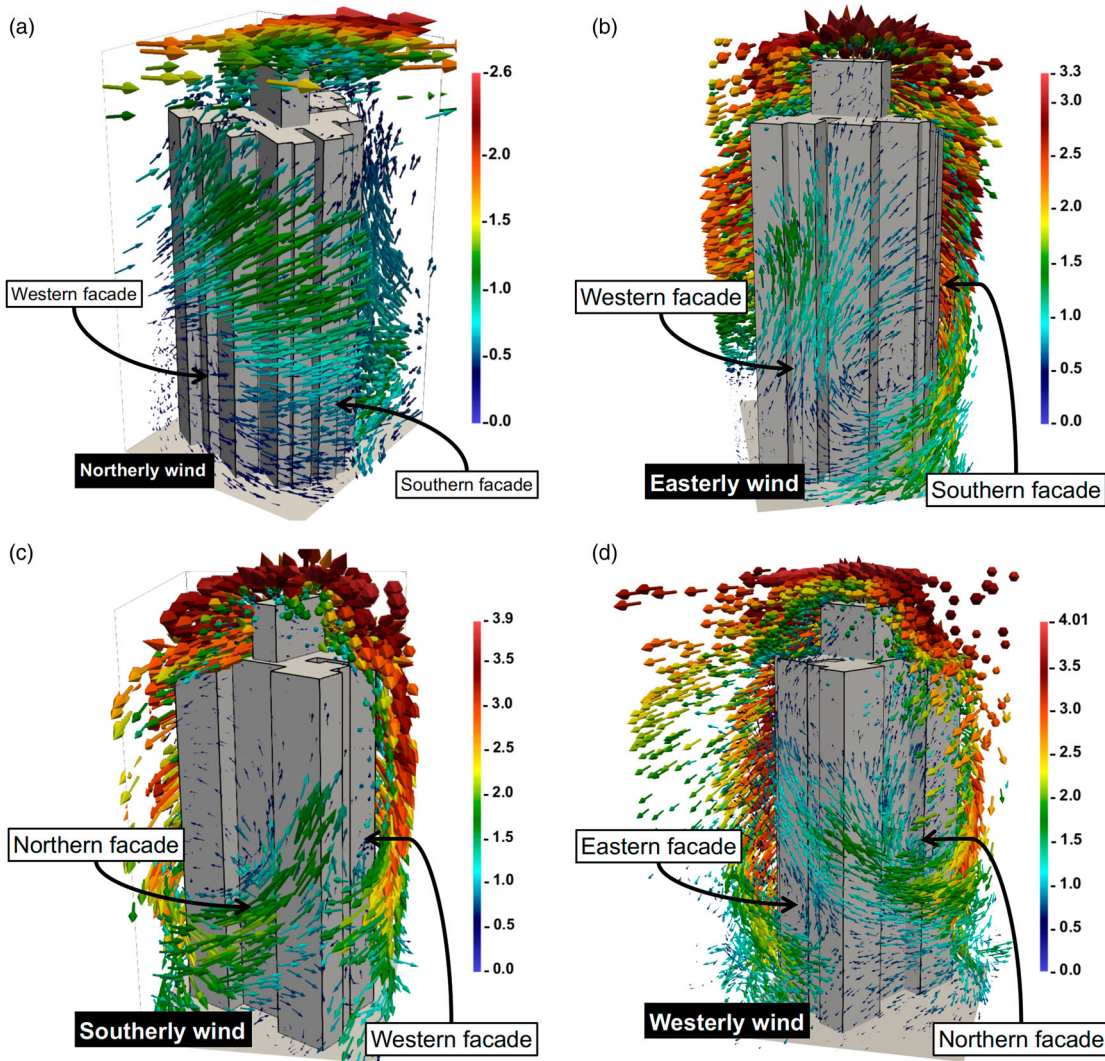


Figure 13. Detailed view of airflow immediately adjacent to the envelope of the Liubo building modelled by FLUIDITY for (a) a northerly wind, (b) an easterly wind, (c) a southerly wind and (d) a westerly wind. Arrows represent the time-averaged velocity vectors. For a northerly wind (a) the western and southern facades of the Liubo building are seen, highlighting that the flow follows the shape of the facades. For an easterly wind (b) a recirculation zone can be observed along the western facade. For a southerly wind, (c) and for a westerly wind (d) a recirculation zone is clearly seen on the northern facade.

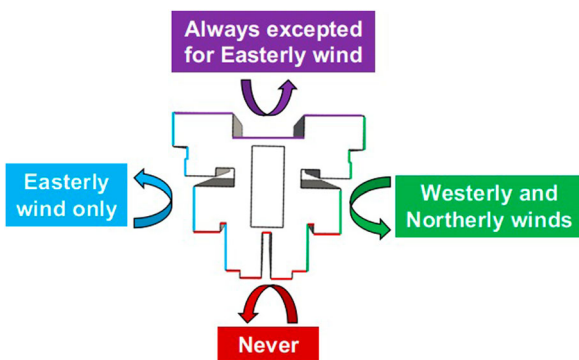


Figure 14. Summary of the main air-recirculation zone around the envelope of the Liubo building.

(ACH) equivalent to $0.15 \text{ m}^3/\text{s}$, 20 ACH equivalent to $0.76 \text{ m}^3/\text{s}$ and 40 ACH equivalent to $1.53 \text{ m}^3/\text{s}$. Internal temperatures can remain below the peak external temperature even when the ventilation is constant through 24 h. Restricting air supply to the minimum 10 l/person/s through the hottest period of an August day simply raises the internal peaks but the model does not factor for cooler supply air within the north re-entrant. Lomas (2007) has reported that 40 ACH are required in temperate climates for ventilation cooling. The potential effect of applying insulation to the exterior of the tower and substituting thermally efficient windows will be the subject of a future paper. At this low latitude there is a risk

that insulation intended to retain more winter heat will conversely reduce the rate at which the building can shed heat in summer and slow the passage of the early afternoon heat flux into the interior, thus extending the overheating period within the day.

In conclusion, the Liubo building is an interesting candidate for the use of natural ventilation located in the HSCW zone. Its northern facade is exposed to vigorous recirculation effects for northerly, southerly and westerly winds. Moreover, for an easterly wind, the air flow is not influenced by the surroundings and the flow remains perfectly aligned with the northern facade (Figure 14). Therefore, the northern facade, which is also the less polluted (Figure 11), presents a good opportunity to catch the wind immediately adjacent to the building, supplying air into the interior of the building whatever the wind direction.

Adaptation proposal

Proposed sun-shading system

The solar geometry was presented above. Effective shading obstructing as close to 100% direct solar radiation (practical at noon on March 21 and September 21 and the summer period between) but permitting useful direct solar gains in winter (November–February) will not be delivered by the ubiquitous horizontal eyebrow shade geometry but a largely vertical zigzag arrangement. The innovative design developed for this condition comprises mesh/perforated aluminium ‘wings’ at 45° in plan. The 45° splay is corrected for the south-south-west orientation with an inclined mesh membrane connecting the wings to intercept the March/September noon projected solar altitude so that all solar gains are excluded through that period 10:00–16:00 hours (Figure 18).

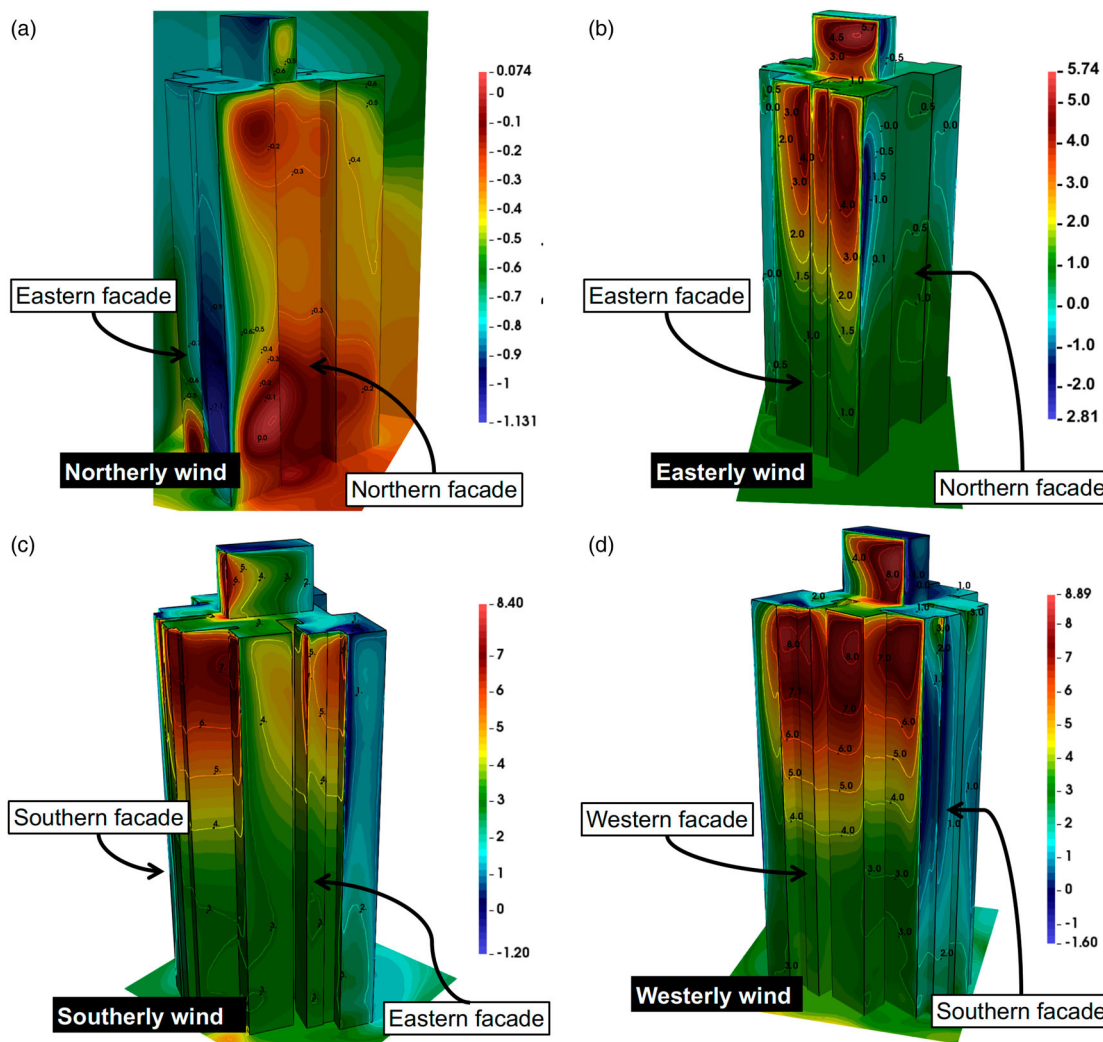


Figure 15. Distribution of the time-averaged relative pressure (Pascals) around the envelope of the Liubo building for (a) a northerly wind, (b) an easterly wind, (c) a southerly wind and (d) a westerly wind. These figures show that the higher pressure values (red values) around the Liubo building are positively correlated with the wind direction. For (b), (c) and (d), the upper part of the building have high pressure because the lower part is shaded by the the surrounding buildings.

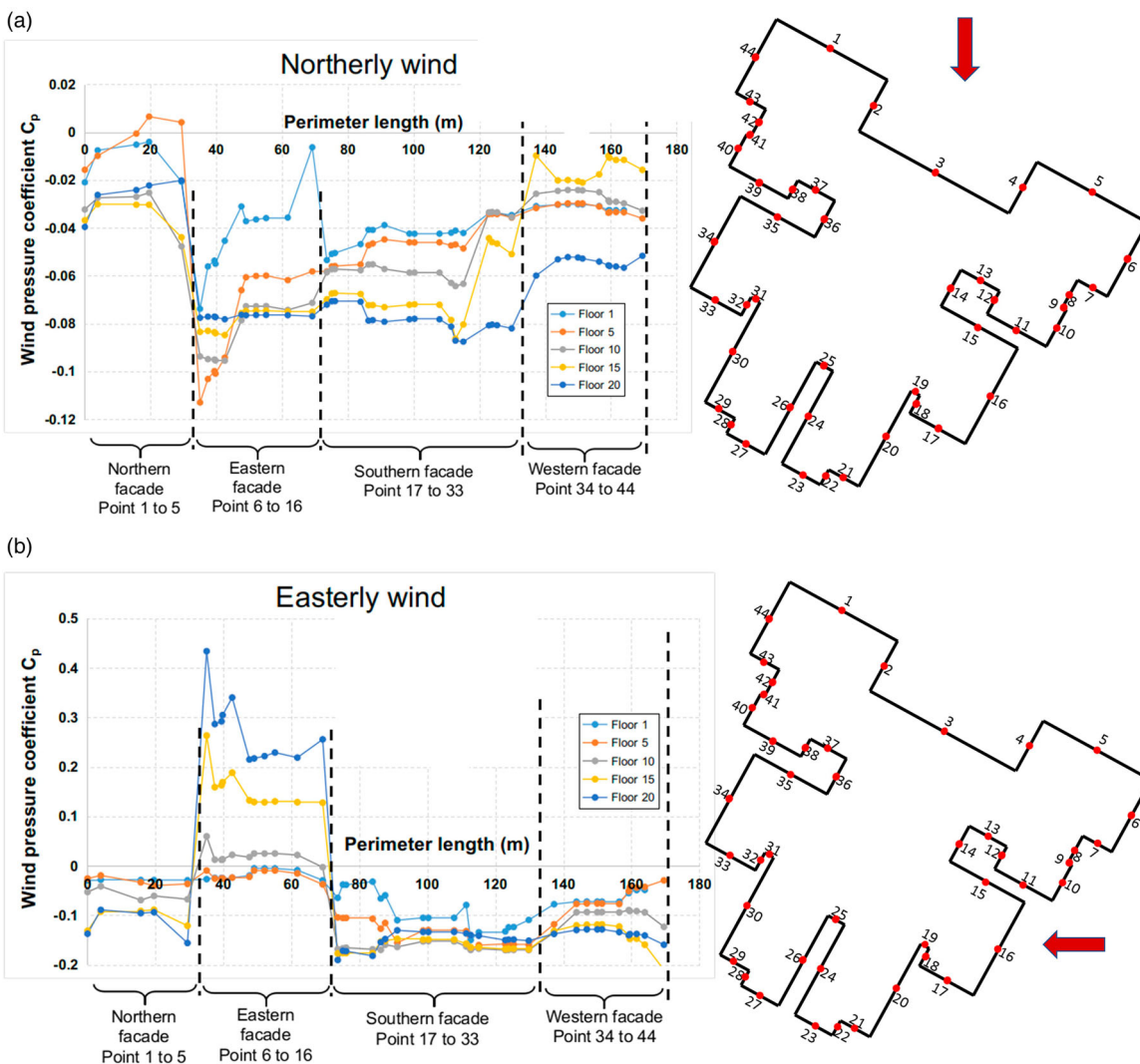


Figure 16. Variation of the wind pressure coefficient ((computed using computational fluid dynamics (CFD) simulations)) along the perimeter of the Liubo building for (a) a northerly wind and (b) an easterly wind and for five different floor levels.

Proposed natural ventilation system

Construction approach

Figure 19(a) is a general arrangement plan locating various adaptation interventions; Figure 19(b) shows the roof level plan. Air intakes designed to intercept airflow around the perimeter of the building are placed to the north in its shadow to supply air at shade temperature. LoHCoil construction partners in Hangzhou suggest the intakes be pre-formed in sections in glass-reinforced concrete (GRC) supported by a steel frame (Figures 20 and 21) with standard insulated connecting ducts into each flat, 900 × 450 mm in section. Air intakes are equipped with dampers to respond to wind direction, which can be fully closed in case of unacceptably high outdoor pollutant concentration levels.

Air is exhausted via insulated ducts of similar cross-sectional area from the balcony enclosures which feed

pre-formed external vertical stacks, also suggested to be pre-formed in the GRC sections (Figure 22). The

Table 1. Wind pressure coefficients, predicted numerically, at the window locations of flats 5 and 6 for four wind directions.

	North	East	South	West	
Wind speed near the flats (m/s)	0.5	0.5	1.0	1.0	
Flat 5	C_p along F4	-0.003	-0.033	-0.170	0.062
	C_p along F5	-0.006	-0.030	-0.190	0.065
	C_p along F6	-0.124	-0.026	-0.070	0.058
	C_p along F7	-0.084	-0.026	-0.010	0.059
	Maximum volume flow rate, Q_{\max} (m ³ /s)	0.0985	0.0249	0.2600	0.0500
Flat 6	C_p along F10	-0.067	-0.027	-0.008	0.261
	C_p along F11	-0.044	-0.023	0.012	0.193
	C_p along F13	-0.046	-0.007	0.018	0.190
	C_p along F14	-0.045	-0.007	0.019	0.191
	Maximum volume flow rate, Q_{\max} (m ³ /s)	0.0468	0.0430	0.1000	0.1700

Note: The estimated flow rate is calculated using equation (1). F4–F7, F10, F11, F13 and F14 stand for the facades' numbers shown in Figure 16.

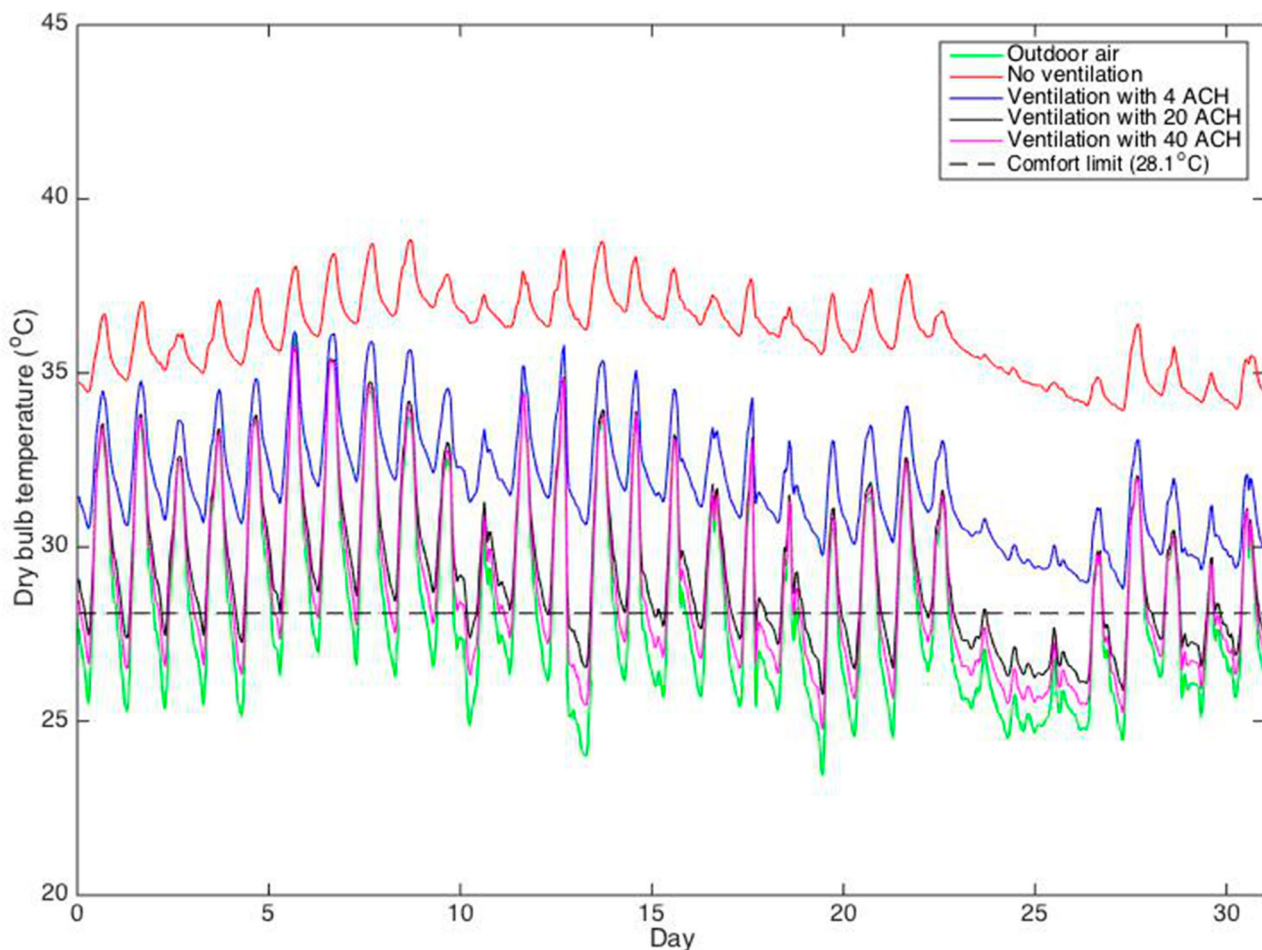


Figure 17. Effect of enabling continuous natural ventilation with increasing air-change rates during the typical meteorological year (TMY) August on indoor air temperature in flat 306.

stack terminations proposed for the Liubo building are 4 m in diameter. The controlled through flow envisaged for the building captures seven pairs of flats per stack segment. The exhaust cross-section areas are matched to the total cross-sectional areas of the 14 supply ducts, based on the authors' practical experience of building large stack-ventilated buildings (Short, Cook, & Lomas, 2009). The stacks are designed to have H-pot/cross-pot terminations to discourage down-draughting, as suggested by Carpenter (1990). Yusoff, Salled, Adam, Sapian, and Sulaiman (2010) report on successful experiments in attracting passive solar gains to heat a stack termination to enhance flow in hot conditions. This is very likely to be necessary in Hangzhou in July and August. The current code governing the minimum distance from nearby buildings is based on access to hours of direct sunlight in a day, the minimum number of hours permitted is two hours at the winter solstice. The fire regulations set another minimum distance constraint of 13 m for a high-rise building (MOHURD code for fire protection

design of buildings GB50016-2014 & Urban residential area planning of the national standard of the People's Republic of China, GB50180-1993). The Liubo building only just satisfies these requirements to east and west but the addition of stacks impinges very locally at the 4 m diameter shaft on these minimum distances to east and west. The authors suggest that policy is altered to enable non-inhabited ventilation infrastructure of minimal width to encroach into this zone. Such stacks will be highly efficient in dissipating smoke from a fire within the interior.

The adaptation proposal is shown in Figure 19 and summarized below (numbers refer to those shown in Figure 19(a)).

The various measures are summarized below.

- Air intake via wind-catcher devices in GRC fixed externally to the north elevation but self-stacking on an internal steel frame, restrained at each slab level. Detailed design proposals for costing in Hangzhou are shown in Figures 20 and 21.

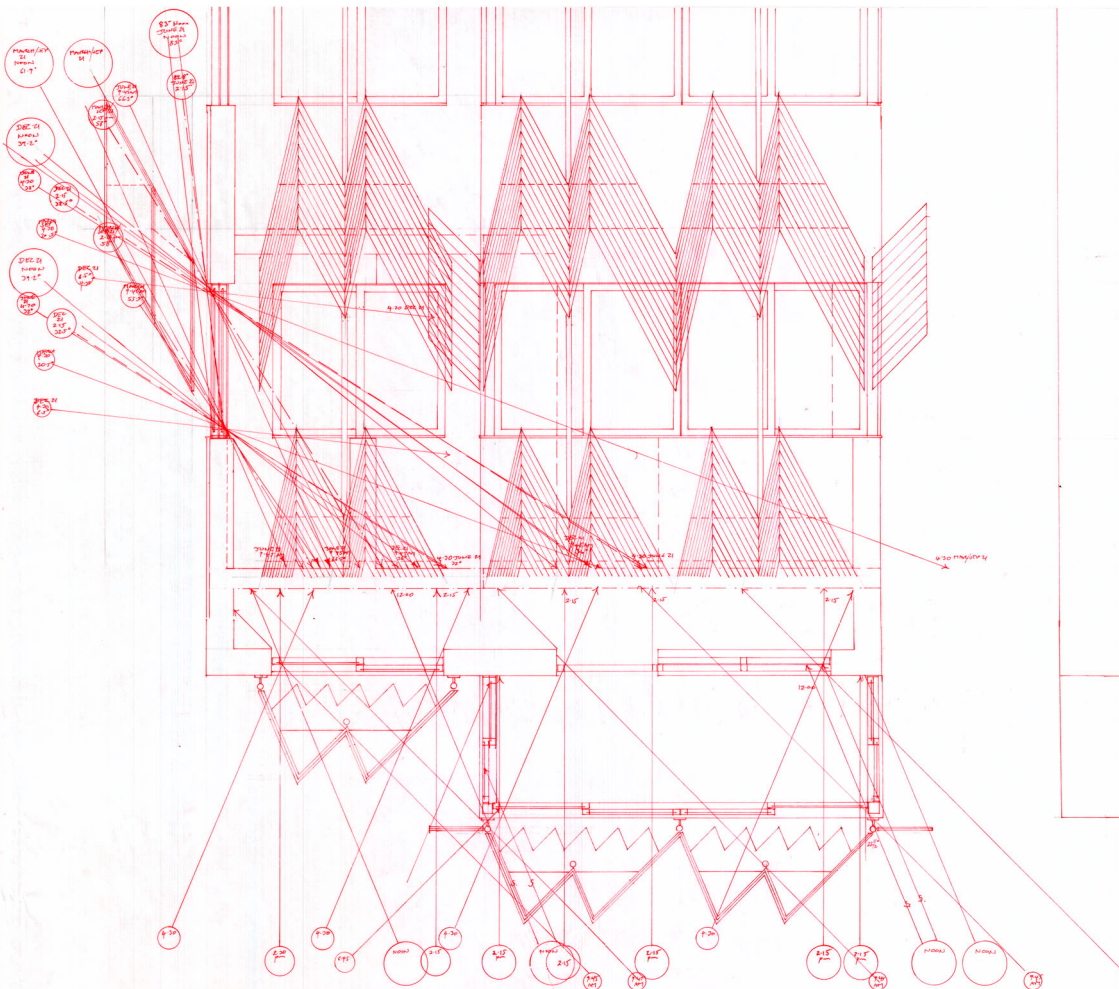


Figure 18. Prototype sun-shading configuration in mesh/perforated aluminium sheet on a steel rectangular hollow section framework to exclude solar gains between April 21 and September 21 without obstructing views out of the building and to have beneficial winter solar gains.

- An air supply duct (900×450 mm internal dimensions) lined in the insulation penetrates the external envelope directing input air from the north side deep into each of eight flats. The dampers are remote operated by a building management system (BMS) but overridden by occupants as required. The complex interaction of occupant and ventilation controls, as discussed above, will be the subject of future research hopefully within a built case study.
 - Each insulated dedicated air supply duct at ceiling level supplies one flat only, delivering air into each flat at the furthest practicable distance from the exhaust entry point.
 - The air supply enters the flat with a fire damper controlled remotely by the alarm system.
 - Exhaust from the flat exits via a remote operated damper with occupant override. Functions as supply in passive downdraught cooling (PDC) reversing flow mode in hot conditions.

- The exhaust stack collects exhaust air from two flats per floor, increasing in cross-sectional area as supplies connect floor by floor. Figure 22 shows exhausts in winter and mid-season mode; Figure S5 in the supplemental data online shows exhausts in PDC mode in hot mid-summer conditions.
 - The outline of slewed exhaust terminations is at mid-tower height.

During the hottest periods the naturally driven system lowers temperatures but cannot maintain temperatures within the comfort zone and so cooling is delivered by reversing flows, generating cooled air at the top of the stacks using cooling batteries and gravity feeding pre-cooled air into the flats, as shown in Figure S5 in the supplemental data online. The horizontal ducts at ceiling level performing as supply ducts in less hot conditions reverse to provide exhaust, the escaping air still cooler than the ambient so stack ventilation will not be effective. The

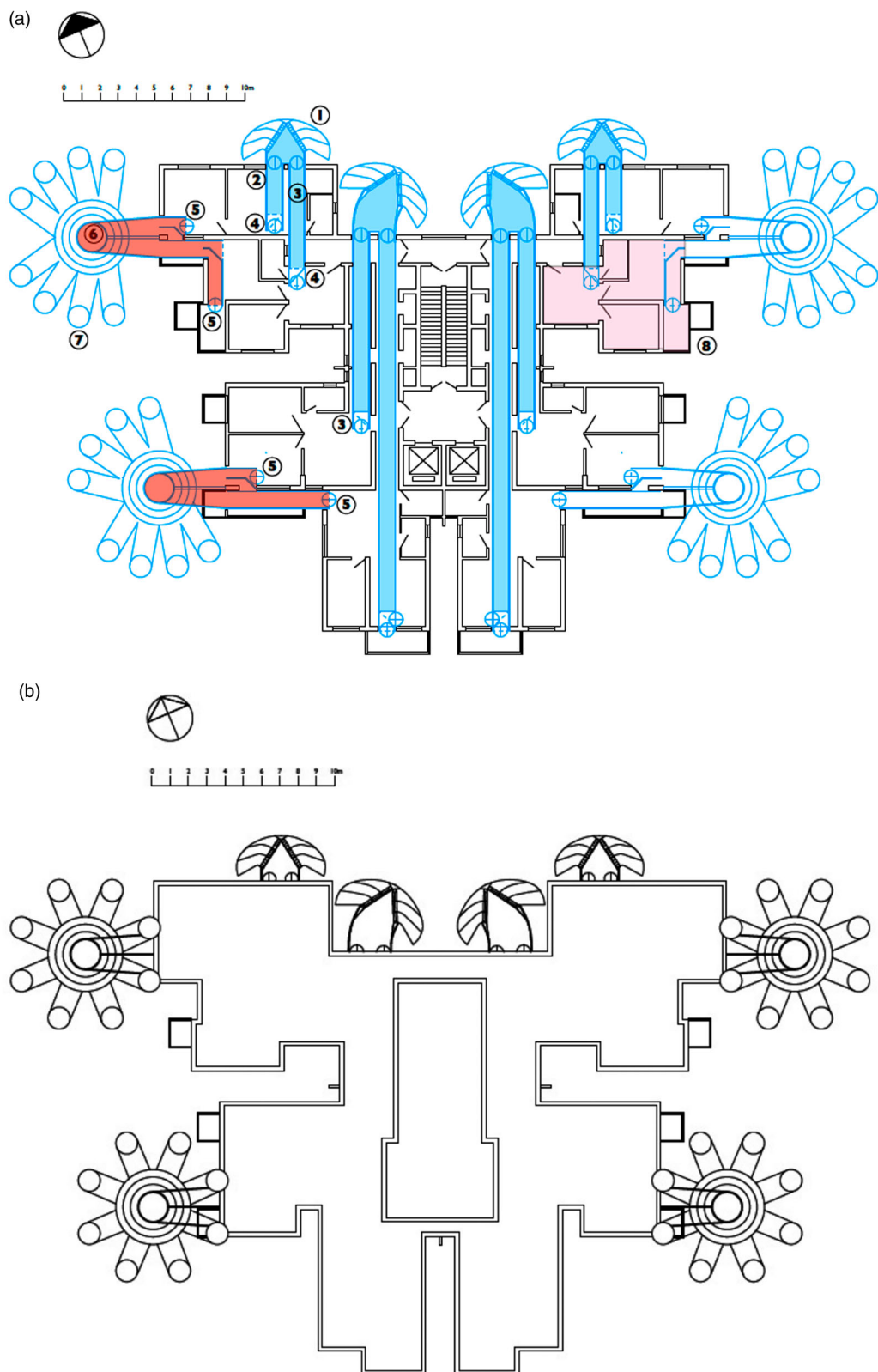


Figure 19. (a) General arrangement of a typical floor plan showing four air intakes applied to the north elevation and four vertical banks of exhaust stacks to the east and west connected into pairs of flats. (b) Roof level plan showing fully developed stack terminations rising above the lift motor room level.

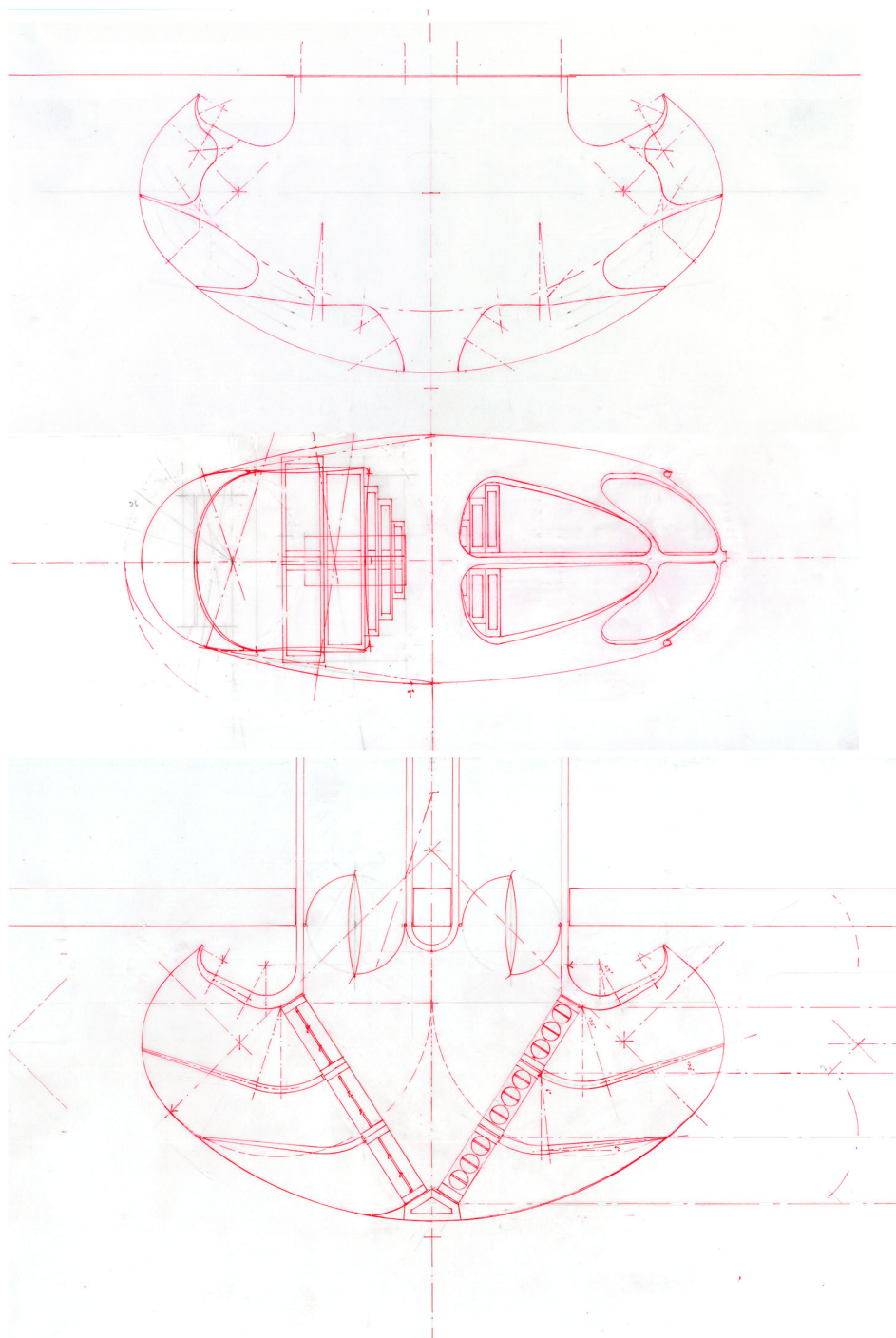


Figure 20. Details of the proposed air intakes formed in GRC: the plan section (top) showing alternating damper positions to respond to the wind direction, both sets open in still air conditions, with the front elevation (centre) and top view (bottom).

LoHCool principal investigator (Short) has experience of achieving successful PDC within the UCL School of Slavonic and East European Studies in Central London (Short, Lomas, & Woods, 2004; Short et al., 2009).

Simulations of indoor airflows

This section explores the potential of the adaptation scheme proposed in the previous section. A simplified

geometry of the whole system was created to run numerical simulations using FLUIDITY (Figure 23). The outdoor air temperature is set to 30°C (in accordance with Figure S1(a) in the supplemental data online). The initial temperature within the flats is also set to 30°C and the floors of the flats are heated to mimic the heat produced by electric devices and occupants. The following results are for a northerly wind.

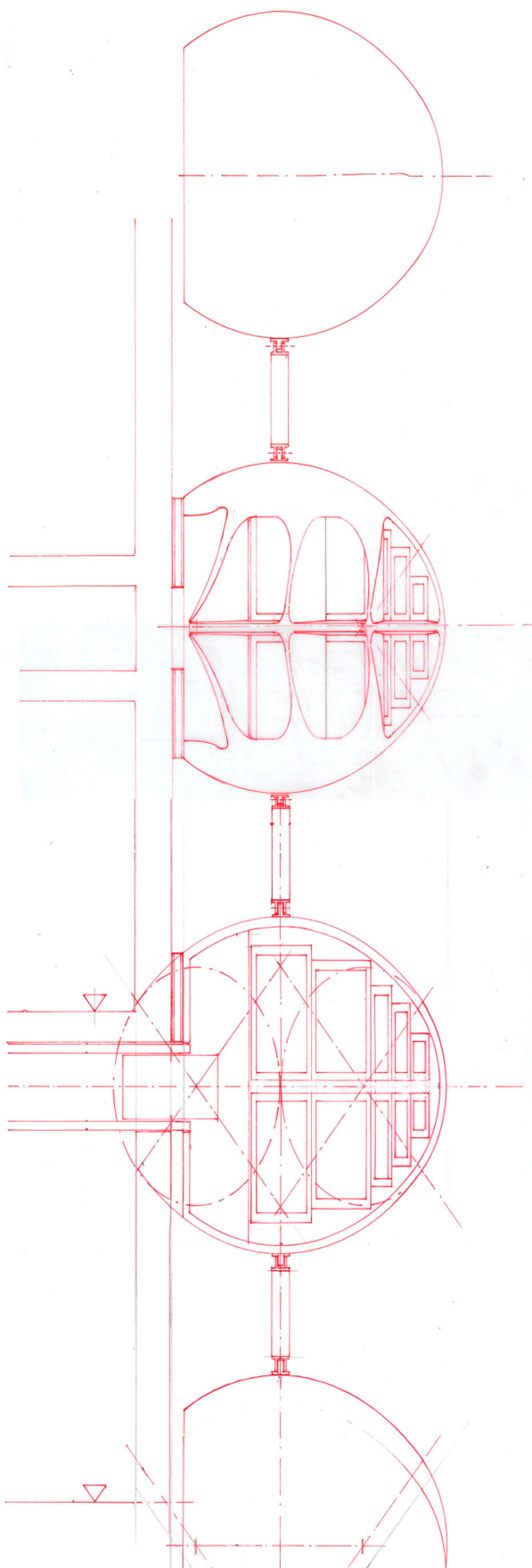


Figure 21. Detail section showing (top) the side elevation of the intake and (bottom) the internal cross-section showing internal dampers.

Figure 24 represents the time-averaged velocity streamlines (curves that are everywhere tangent to the velocity vector) and the time-averaged velocity vectors within flats 5 and 6 on a typical lower floor for a north-easterly wind. Note that the scale in Figure 24 is between 0 and 0.1 m/s to better see the colour gradient, but the air speed can reach 0.15 m/s. Air mixing, characterized by vortexes, in every room of flats 5 and 6 is clearly observed in Figure 24. For both flats, the flow path of the air from the intake towards the exhaust is characterized by speeds higher than 0.08 m/s, with maximums of 0.15 m/s: the air enters in the living room, then enters the bedroom and escapes via the balcony. The instantaneous spatially averaged air speed in the living room is shown in Figure 25. The air speed in both living rooms is relatively low, with time averages of 0.036 m/s for flat 5 and 0.021 m/s for flat 6 and maximums of 0.091 m/s for flat 5 and 0.044 m/s for flat 6, meaning that residents will not feel any uncomfortable draught.

For a northerly wind, occasionally, reversed flow occurs in the pipe linked to flat 6, as shown in Figure S6 in the supplemental data online. These events, which happen when the air intake fails to catch enough wind, are so short in time (1 or 2 s maximum) that the flow has no time to be fully established and thus does not impact the indoor air quality.

The ventilation flow rate predicted from CFD simulations as a function of time is shown in Figure 26. The inlet flow rate is lower than zero four times during the time slot plotted, corresponding to a reversed flow episode (see Figure S6 in the supplemental data online). The time-averaged ventilation flow rate at the inlet of the intake pipe is $0.13 \text{ m}^3/\text{s}$ for flat 5 and $0.076 \text{ m}^3/\text{s}$ for flat 6. The comparison between these time averages and the maximum ones (without the adaptation scheme) predicted in Table 1 highlight that the proposed adaptation scheme can increase the ventilation flow rate by about 31.9% for flat 5 and by 63.3% for flat 6. The maximum inlet ventilation rate during the period shown in Figure 26 is $0.38 \text{ m}^3/\text{s}$ for flat 5 and $0.2 \text{ m}^3/\text{s}$ for flat 6.

The time-averaged velocity vectors in the stack chimney are shown in Figure 27(a), highlighting that the stack chimney can evacuate the air towards the outdoors. An air-recirculation zone can be observed at the bottom of the stack, however the stack can bring the flow up towards the top of the chimney. An example of the instantaneous velocity vectors (at time $t = 1600 \text{ s}$) at the top of the chimney is shown in Figure 27(a) to see how the flow behaves near the termination. Figure 27 highlights the fact that the air within the chimney can be evacuated through the H-pot termination proposed in the adaptation scheme with no obvious downdraughting near the cowl and the termination. Figure 27(b)

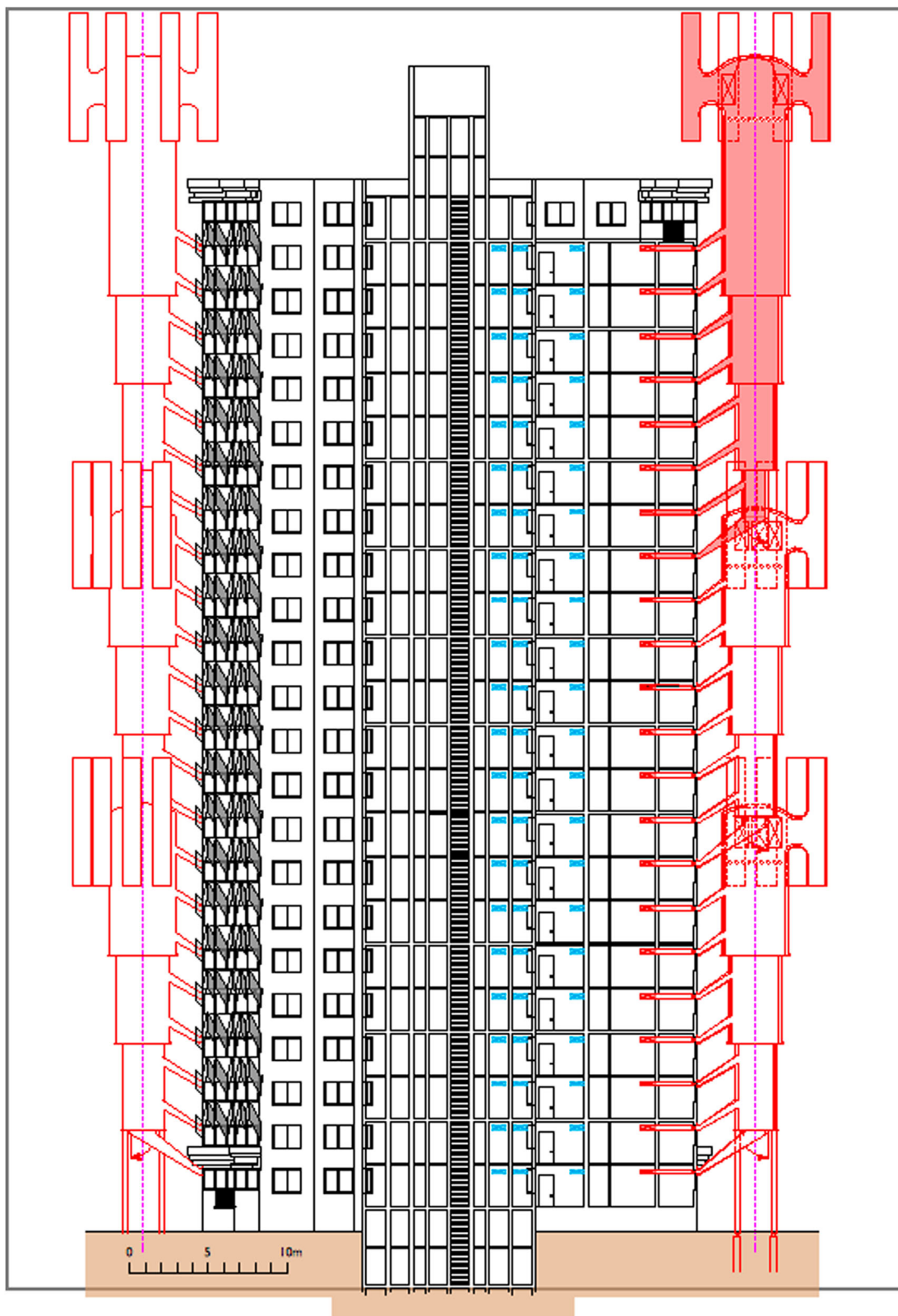


Figure 22. East–west section showing the northernmost exhaust stacks in precast GRC connected into seven pairs of flats per stack, organized in three load-bearing vertical assemblies restrained by the tower at slab levels.

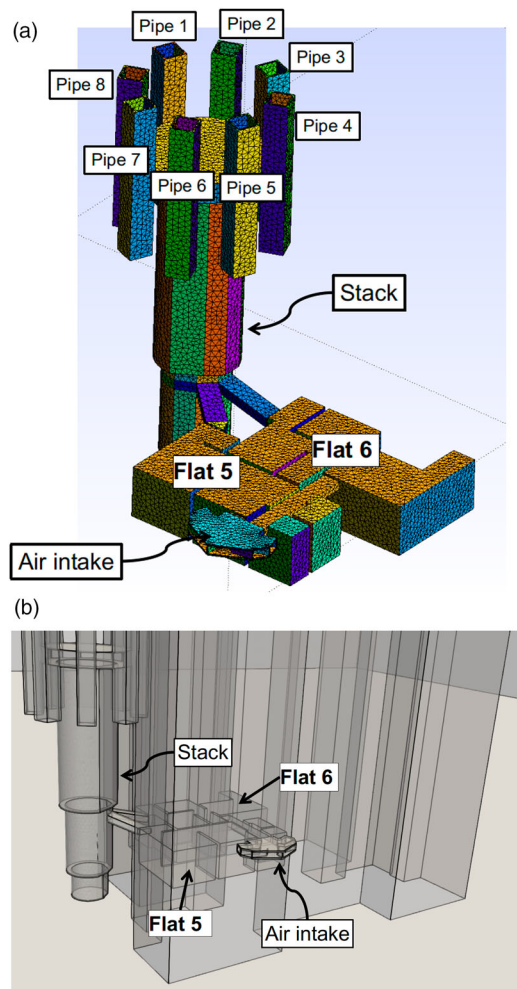


Figure 23. Full assembly of intake, supply ducts, flat volume, ducts to the exhaust stack, the stack and a full termination as modelled in FLUIDITY: (a) geometry and mesh of flats 5 and 6, the intake and the exhaust stack; and (b) the fully coupled indoor–outdoor geometry with the adaptation proposed in this paper.

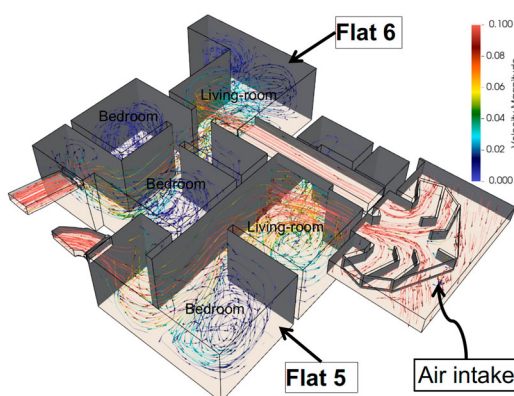


Figure 24. Prediction of air flow patterns (velocity streamlines and velocity vectors) within flats 5 and 6 using the FLUIDITY model for a northerly wind. Results are time averaged.

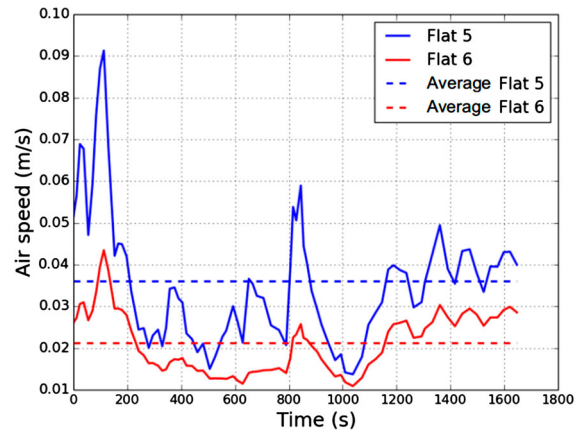


Figure 25. Spatially averaged air speed in the living rooms of flats 5 and 6 for a northerly wind.

shows that the air escaping the stack is not evacuated uniformly in each pipe. In that particular time ($t = 1600$ s), it is also interesting to note that the outdoor air can enter the stacks (pipe 1 in Figure 27(b)), while the air within the stack is well evacuated (through the pipes 2–4, 6 and 8).

To test whether the stack performs its role correctly, the air flow rate escaping the chimney through each pipe (through the surfaces shown in Figure 27(b)) and the total flow rates are shown in Figure 28: negative values mean there is more air entering the stack than air escaping; positive values mean there is more air escaping the stack than entering. The time averages for flow rate through each pipe are $0.13 \text{ m}^3/\text{s}$ (pipe 1), $-0.02 \text{ m}^3/\text{s}$ (pipe 2), $0.08 \text{ m}^3/\text{s}$ (pipe 3), $0.01 \text{ m}^3/\text{s}$ (pipe 4), $-0.097 \text{ m}^3/\text{s}$ (pipe 5), $0.005 \text{ m}^3/\text{s}$ (pipe 6), $0.02 \text{ m}^3/\text{s}$ (pipe 7) and $0.01 \text{ m}^3/\text{s}$ (pipe 8). From Figure 28(a) and the values above, it is clear that the air within the stack is mainly evacuated through pipes 1 and 3, while outside air enters through pipes 5 and 2. Averaged over time, the

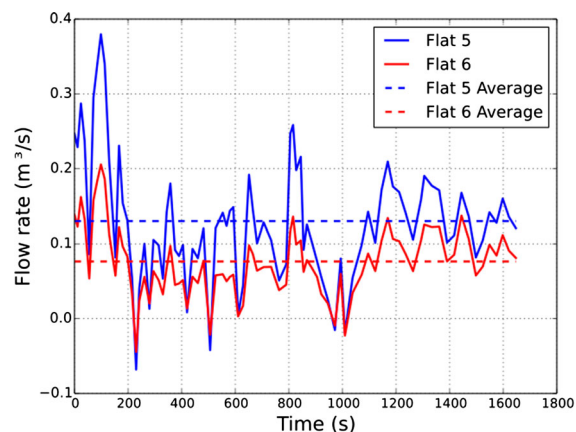


Figure 26. Ventilation flow rate at the intake for flats 5 and 6 under a northerly wind.

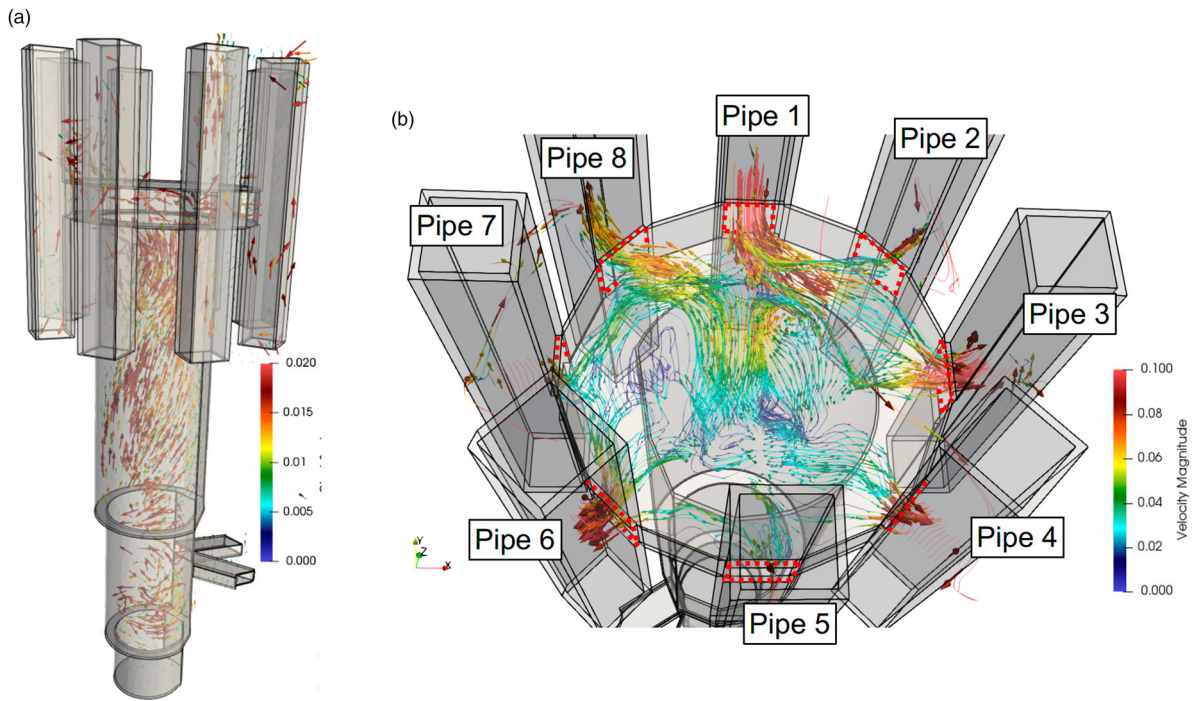


Figure 27. (a) Time-averaged velocity vectors in the stack; and (b) streamlines and velocity vectors at 1600 s at the top of the chimney near the cowl for a northerly wind. The dashed red lines depict the surface where the air flow rate is computed.

other pipes (4 and 6–8) contribute less to the evacuation of air. Even if outside air can enter the stack, the total flow rate (Figure 28(b)) stays mostly positive, with a time average of $0.15 \text{ m}^3/\text{s}$, meaning that the air within the stack is well evacuated towards the outside. The few episodes where the total mass flow is lower than zero (Figure 28(b)) can be correlated with the ‘reversed’ episodes described previously (Figure 26 and see Figure S6 in the supplemental data online).

The PMV is computed using Fanger’s (1970) theory set against the ASHRAE criteria. The total range of the PMV is between -3 and 3 and it can be interpreted as follows: -3, people feel cold; -2, people feel cool; -1, people feel slightly cool; 0, people feel neutral; 1, people feel slightly warm; 2, people feel warm; and 3, people feel hot. The outdoor humidity is taken equal to 80% (in accordance with Figure S1(b) in the supplemental data online) and it is assumed that people wear one unit of cloth. The iso-surfaces (the surface representing points of a constant value) of the PMV equal 0 (in blue), 1 (in green) and 2 (in red) and are shown in Figure S7 in the supplemental data online for flats 5 and 6 and for a northerly wind. It can be seen that people feel between neutral and warm, meaning they feel relatively comfortable in both flats. The hottest regions within the flats are near the floor because the floor is heated to mimic the heat produced by electric devices, explaining why people feel warmer in the lower part of the flats. These results are based on Fanger’s theory. However, based on the

discussion above, it is expected that people will feel even more comfortable against the HSCW zone criteria developed by Li and Yao (2012).

The inlet ventilation flow rate predicted from CFD simulations is still quite low compared with values expected for natural ventilation using a wind and stack-assisted adaptation scheme. However, this can easily be explained by the following. The results presented in this section come from a simplified geometry of the adaptation scheme proposed in the previous section. Indeed, the intake is fully opened: there are no dampers responding to wind direction. Hence, the caught air can escape the intake through the opposite openings (Figure 24 and see Figure S6 in the supplemental data online) inducing a loss of air flow which should normally feed the flats. Moreover, only one pair of flats is connected to the stack, while the stack is dimensioned for seven pairs of flats. The dampers and all the flats will be added in the simulation in further work. The stack modelled is the most disadvantaged of the three vertically arranged stacks. The lowest stack modelled is the lowest of the three vertically arranged stacks.

The LoHCool researchers believe this is the first time that this kind of simulation, using LES, coupling indoor and outdoor space in such a complex geometry has been attempted. The first results are promising and highlight that such a system as the one proposed here can generate flows capable of achieving good mixing of air within groupings of flats when using natural ventilation.

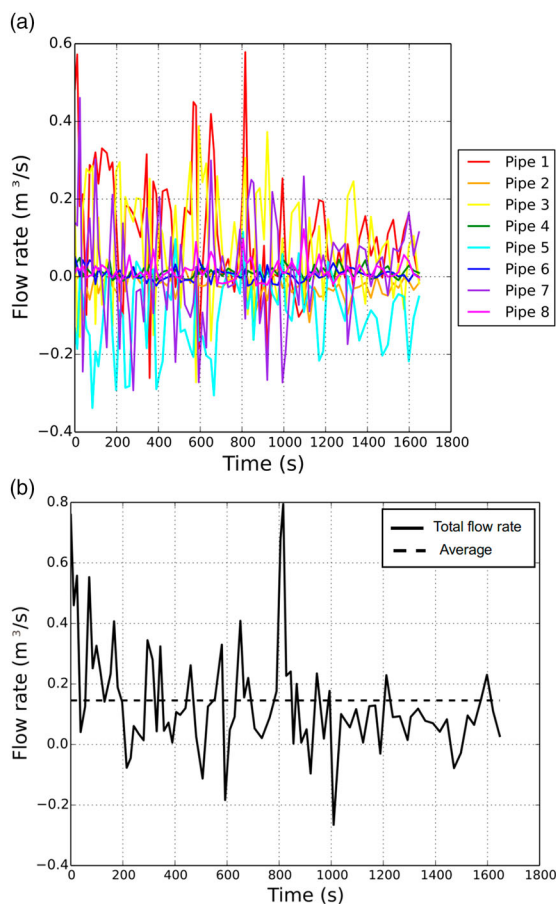


Figure 28. (a) Air flow rate escaping the chimney through each pipe (through the surfaces shown in Figure 27(b)); and (b) total flow rate for a northerly wind. Negative values mean there is more air entering the stack than air escaping; positive values mean there is more air escaping the stack than air entering.

Commentary on the implementation in Zhejiang province

LoHCool project construction industry partners Hangzhou Zhengzai Architecture Design and Research Institute Co. Ltd confirm that their favoured construction method for the ventilation towers is to use GRC with a skeletal steel support structure. They advise each tower may cost in the order of RMB700,000 (US\$107,128). (The exchange rate for RMB to US\$ is taken as 0.15304 – the yearly average rate between June 2017 and May 2018; oanda.com.) For the wind catchers and external vent pipes, they suggest the use of stainless steel and aluminium for the connecting vent ducts, estimating that each wind catcher may cost RMB30,000 (US\$4591) and that the vent pipe (diameter of 300 mm) will cost about RMB100/m installed (US\$60/m). As such, each floor may cost in the order of RMB158,000 (US\$24,180), suggesting a total

construction cost of RMB5,867,200 (US\$897,916) in total, some RMB514/m² (US\$79/m²), including labour costs, for the whole adaptation scheme.

The installation of a conventional centralized AC system was also scoped and costed. A future productive life for the tower of 30 years is assumed pending either solution. The industry partner advises that AC sized to contemporary Chinese standards to achieve the comfort conditions prescribed by central government as outlined above would be installed floor by floor at a cost of RMB80,000 (US\$12,243) per floor, some RMB1.84 million (US\$281,594) in total, RMB161.2/m² (US\$24.7/m²). Some floor space would be lost per floor. Additional plant room space on the roof would cost RMB3000/m² (US\$459/m²). The plant would require replacement in 15 years so that in 30 years some RMB3.68 million (US\$563,187) will require to be expended on the replacement of the AC plant. An annual maintenance budget per floor is difficult to predict but RMB500 (US\$77) per floor per year seems reasonable, giving an annual budget for the building of RMB11,500 (US\$1760), RMB0.94/m² (US\$0.14/m²). A similar budget is envisaged for the natural ventilation scheme in inspecting and repairing dampers and controls. The annual energy cost for the AC system at RMB0.54/kWh (US\$0.08/kWh) is predicted to be of the order of RMB268,000 (US\$41,015), or RMB21.96/m² (US\$3.36/m²).

Very crudely at today's prices, the difference in construction cost over a 30-year life would be:

$$[\text{RMB}5.8672 \text{ million (US\$897,916)} \text{ natural ventilation construction} + \text{RMB}0.345 \text{ million (US\$52,799)} \text{ maintenance}] - [\text{RMB}1.84 \text{ million (US\$281,594)} \text{ for AC installation} + \text{RMB}1.84 \text{ million (US\$281,594)} \text{ replacement at half-life} + \text{RMB}0.345 \text{ million (US\$52,799)} \text{ maintenance}] = \text{a difference of RMB}2.192 \text{ million (US\$335,464)}$$

leading to an energy cost saving over 30 years of:

$$\text{RMB}0.268 \text{ million (US\$41,015)} \times 30 \text{ years} = \text{RMB}8.04 \text{ million (US\$1,224,381)}$$

Without accounting for discount rates (currently 8% in China), the price rise index or multiplier at today's prices, the payback is 8.18 years, suggesting that the proposed natural ventilation alternative is within the realm of viability. Perhaps more importantly given the aims of the LoHCool project and the Chinese government's policy it seeks to inform and assist is the estimated saving in carbon emissions of 389,140 kg/year, equivalent to 34.1 kg/m²/year of occupied floor area and a cumulative total of 11.674 million kg over 30 years.

Conclusions

The LoHCool work in Hangzhou has provided opportunities to consider the adaptation potential of relatively recent apartment towers in a challenging climate in which the key carbon-reduction challenge is shown to be in the reduction of summer cooling loads and therefore to develop options other than the sealing and full AC of the building as living standards and expectations continue to grow at a rate unprecedented in the West in recent memory. A series of thermal and airflow modelling exercises in conjunction with the collection of environmental performance data has enabled a diagnosis of the summer overheating problem in terms of direct solar gains, internal gains, ventilation and air movement, orientation and climate, and the generation of re-engineering options to ameliorate internal overheating.

The design interventions are concentrated externally to minimally disrupt the internal life of the building and its occupants and its integral fire safety. Initial costings and feasibility work supporting the proposals (in comparison with full AC) show that the proposed adaptation measures as a holistic strategy are sufficiently viable to warrant further exploration. The potential savings in carbon emissions are prodigious. The case study building has been considered in its full urban context of high- and medium-rise buildings using LES simulations. This is essential to generate reliable results. The height and pattern of neighbouring buildings is shown to be highly influential on the subject tower's performance and future work will explore further the effect of groups of tall buildings on each other. The case study building is modelled with a pollutant source nearby and is shown to be vulnerable to concentrations above a C_{max} of 1% under northerly wind conditions and only for the lower part of the tower. The intakes on the north side are never exposed to pollution levels above a C_{max} of 1%, demonstrating that natural ventilation design, closely informed by CFD simulations, can achieve viable but closely tailored solutions in city environments. The complex adaptation scheme proposed in this paper has been studied numerically under a northerly wind highlighting that a new design can be an effective solution for industry standard interventions.

In the context of cities in China, air quality will be continue to be an important determinant of the potential benefit or otherwise of advanced natural ventilation schemes until air quality measures take full effect. Indeed, air quality is the central theme of the associated project MAGIC. At the urban scale, this research suggests that optimizing the height of the buildings could be a major factor in urban design as this affects the balance of outdoor-indoor pollution and temperature interactions and

subsequently the energy efficiency of buildings. Zhejiang University has modelled traffic movement and volume in this neighbourhood of Hangzhou and there is an ambition to incorporate that traffic model into the FLUIDITY model to enable the prediction of ventilation cooling potential incorporating an indication of air quality. The Anglo-Chinese research team very much hopes to see related adaptation schemes built and closely monitored in order to advance the understanding of alternative very low-carbon approaches to delivering built environments to satisfy increasing comfort aspirations.

Acknowledgements

The authors are extremely grateful to the Low Carbon Climate-Responsive Heating and Cooling of Cities (LoHCool) project partners for their continuing and active support, based in China and the UK. In Hangzhou: the Hangzhou Municipal Construction Commission; the Department of Housing and Urban-Rural Development of Zhejiang Province; the Zhejiang Province Construction Technology Promotion Center; and the Zhejiang Shimao Real Estate Group. In Chongqing: the Chongqing Municipal Commission of Urban-Rural Development; the Chongqing Green Building Council; and the Chongqing Construction Engineering Group Development and Management Co. Ltd. More recently recruited partners include the Hangzhou Zhengzai Architecture Design and Research Institute Co. Ltd; The China Third Nantong Construction Company; and the Yibin Grace Group Co. The Chinese national institutions that generously supported the project include: The Ministry of Housing Urban and Rural Development (MOHURD); the Centre of Science and Technology in Construction; The China Green Building Council; The China Academy of Building Research in Beijing; the MOHURD China Association of Building Energy Efficiency; the Shanghai Research Institute of Building Sciences; the Shenzhen Institute of Building Research; the China Southwest Architectural Design and Research Institute; and the MOST National Center for International Research of Low-carbon & Green Buildings, for which the lead author is International Co-Director. In the UK, project partners included: AECOM Ltd (UK); Buro Happold; Skanska UK PLC; ARCC; SPIE Ltd (UK); Building Design Partnership (BDP); Screenspace Productions Ltd; and The Chartered Institute of Building (CIOB). The LoHCool Project Administrator was Beau Brady-Patel, based at the University of Cambridge.

Disclosure statement

No potential conflict of interest was reported by the authors.

Funding

The authors are most grateful to the UK Engineering and Physical Sciences Research Council (EPSRC) and the National Natural Science Foundation of China (NSFC) for funding the collaborative multidisciplinary project Low Carbon Climate-Responsive Heating and Cooling of Cities (LoHCool) [NSFC

grant number 51561135002; and EPSRC grant number EP/N009797/1]. The full research team comprised the University of Cambridge's departments of Architecture and Engineering; Chongqing University; Zhejiang University; the University of Reading; the University of Cambridge's Institute of Atmospheric Physics; and Loughborough University's Department of Civil and Building Engineering. LoHCool also benefitted from a close collaboration with the EPSRC Grand Challenges project 'Managing Air for Green Inner Cities' (MAGIC) [EPSRC reference number EP/N010221/1], in which the projects shared two research associates equally so that LoHCool China Case Studies were available to MAGIC and benefitted from modelling capability at Imperial College London. MAGIC is led by the Department of Applied Mathematics and Theoretical Physics, University of Cambridge, with Imperial College's Department of Earth Science and Engineering, the departments of Engineering, Architecture, Geography, Chemistry and Land Economy at the University of Cambridge, and the universities of Surrey and Reading.

ORCID

- C. Alan Short  <http://orcid.org/0000-0001-5699-0259>
 Jiyun Song  <http://orcid.org/0000-0002-9483-0501>
 Laetitia Mottet  <http://orcid.org/0000-0002-0381-7521>

References

- Aflaki, A., Mahyuddin, N., Mahmoud, Z. A. C., & Baharum, M. R. (2015). A review on natural ventilation applications through building façade components and ventilation openings in tropical climates. *Energy and Buildings*, 101, 153–162.
- AMCG, Fluidity manual v4.1.12. (2015). Imperial College London.
- Aristodemou, E., Bentham, T., Pain, C., & Robins, A. (2009). A comparison of mesh-adaptive LES with wind tunnel data for flow past buildings: Mean flows and velocity fluctuations. *Atmospheric Environment*, 43, 6238–6253.
- Aristodemou, E., Bogenegra, L. M., Mottet, L., Pavlidis, D., Constantinou, A., Pain, C., & ApSimon, H. (2018). How tall buildings affect turbulent air flows and dispersion of pollution within a neighbourhood. *Environmental Pollution*, 233, 782–796.
- Asfour, O. S., & Gadi, M. B. (2007). A comparison between CFD and network models for predicting wind-driven ventilation in buildings. *Building and Environment*, 42, 4079–4085.
- ASHRAE. (2004). Thermal environmental conditions for human occupancy. ASHRAE Standard 55-2004, Atlanta, Georgia, American Society of Heating, Refrigerating and Air-Conditioning Engineers.
- Bentham, T. (2003). *Microscale modelling of air flow and pollutant dispersion in the urban environment* (PhD thesis). Imperial College London.
- Blocken, B. (2014). 50 years of computational wind engineering: Past, present and future. *Journal of Wind Engineering and Industrial Aerodynamics*, 129, 69–102.
- Blocken, B., Van Hooff, T., Aanen, L., & Bronsema, B. (2011). Computational analysis of the performance of a Venturi-shaped roof for natural ventilation: Venturi-effect versus wind-blocking effect. *Computers and Fluids*, 48, 202–213.
- Carpenter, C. J. (1990). The effectiveness of anti-downdraught domestic chimney pots in preventing smoke blow-back. *Journal of Wind Engineering and Industrial Aerodynamics*, 34, 147–168.
- Carrilho Da Graca, G., Chen, Q., Glicksman, L. R., & Norford, L. K. (2002). Simulation of wind-driven ventilative cooling systems for an apartment building in Beijing and Shanghai. *Energy and Buildings*, 34, 1–11.
- Chen, Q. (2009). Ventilation performance prediction for buildings: A method overview and recent applications. *Building and Environment*, 44, 848–858.
- Chenari, B., Carrilho, J. D., & Gameiro Da Silva, M. (2016). Towards sustainable, energy-efficient and healthy ventilation strategies in buildings: A review. *Renewable and Sustainable Energy Reviews*, 59, 1426–1447.
- Cheung, J. O. P., & Liu, C. H. (2011). CFD simulations of natural ventilation behaviour in high-rise buildings in regular and staggered arrangements at various spacings. *Energy and Buildings*, 43, 1149–1158.
- China Urban Research Committee (CURC). (2008). *Green building*. Beijing: Architecture and Building Press. [in Chinese]
- Chiu, Y. H., & Etheridge, D. W. (2007). External flow effects on the discharge coefficients of two types of ventilation opening. *Journal of Wind Engineering and Industrial Aerodynamics*, 95, 225–252.
- Chow, D. H. C., Li, Z., & Darkwa, J. (2013). The effectiveness of retrofitting existing public buildings in face of future climate change in the hot summer cold winter region of China. *Energy and Buildings*, 57, 176–186.
- Chu, C. R., & Chiang, B. F. (2013). Wind-driven cross ventilation with internal obstacles. *Energy and Buildings*, 67, 201–209.
- CMA. (2005). *Meteorological Information Center of the China Meteorological Administration and the Department of Building Technology & Science of Tsinghua University. China meteorological data collection for building thermal environment analysis*. Beijing: China Architecture and Building Press. [in Chinese]
- Cole, R. (2012). Regenerative design and development: Current theory and practice. *Building Research & Information*, 40(1), 1–6. doi:10.1080/09613218.2012.617516
- Costanzo, V. (2017). Estimating urban buildings' Energy Use Intensities (EUIs) by means of a bottom-up multi-layer engineering approach, 8th International Conference on Sustainable Development in Building and Environment (SUDBE) Conference.
- Dawson, R. (2007). Re-engineering cities: A framework for adaptation to global change. *Philosophical Transactions of the Royal Society A: Mathematical, Physical and Engineering Sciences*, 365, 3085–3098.
- Debay, J. E. (2017). *Natural ventilation of buildings: Efficiency assessment with CFD* (Master's Thesis). University of Cambridge and Institut National des Sciences Appliquées de Paris.
- de Dear, R. J., & Brager, G. S. (1998). Developing an adaptive model of thermal comfort and preference. *ASHRAE Transactions*, 104, 145–167.
- Dixon, T., & Eames, M. (2013). Scaling up: The challenges of urban retrofit. *Building Research & Information*, 41(5), 499–503. doi:10.1080/09613218.2013.812432
- EnergyPlus, U.S. Department of Energy. (2017). Engineering reference of EnergyPlus Version 8.8 documentation.

- Essah, E. A., Yao, R., & Short, A. (2017). Assessing stack ventilation strategies in the continental climate of Beijing using CFD simulations. *International Journal of Ventilation*, 16, 61–80.
- Fanger, P. O. (1970). *Thermal comfort*. Copenhagen: Danish Technical Press.
- Ford, R., Pain, C. C., Piggott, M. D., Goddard, A. J. H., de Oliveira, C. R. E., & Umpleby, A. P. (2004). A nonhydrostatic finite-element model for three-dimensional stratified oceanic flows. Part I: Model formulation. *Monthly Weather Review*, 132, 2816–2831.
- Ge, J., Wu, J., Chen, S., & Wu, J. (2018). Energy efficiency optimization strategies for university research buildings with hot summer and cold winter climate of China based on the adaptive thermal comfort. *Journal of Building Engineering*, 18, 321–330.
- Ge, J., & Yu, Z. (2016). Methodology to select the typical buildings. Zhejiang University Department of Architecture, LoHCool Working Paper, unpublished.
- Giridharana, R., Lomas, K. J., Short, C. A., & Fair, A. J. (2013). Performance of hospital spaces in summer: A case study of a 'Nucleus'-type hospital in the UK midlands. *Energy and Buildings*, 66, 315–328.
- Guo, W., Liu, X., & Yuan, X. (2015). Study on natural ventilation design optimization based on CFD simulation for green buildings. *9th International Symposium on Heating, Ventilation and Air Conditioning (ISHVAC) and the 3rd International Conference on Building Energy and Environment (COBEE)*, Procedia Engineering (121, pp. 573–581).
- Hajdukiewicz, M., Geron, M., & Keane, M. M. (2013). Calibrated CFD simulation to evaluate thermal comfort in a highly-glazed naturally ventilated room. *Building and Environment*, 70, 73–89.
- Hall A. (1880). Hall's patent ventilator and chimney-cowl. *The Lancet*, 116(2977), 462. Retrieved from <https://www.sciencedirect.com/science/article/pii/S0140673600329889?via%3Dihub>
- Hesse, F. (2017). *Large eddy simulation of buoyancy-driven flows: Plumes and natural building ventilation* (Master's thesis). Imperial College London.
- Ho, M. C., Chiang, C. M., Chou, P. C., Chang, K. F., & Lee, C. Y. (2008). Optimal sun-shading design for enhanced daylight illumination of subtropical classrooms. *Energy and Buildings*, 40, 1844–1855.
- Hughes, B. R., Calautit, J. K., & Ghani, S. A. (2012). The development of commercial wind towers for natural ventilation: A review. *Applied Energy*, 92, 606–627.
- Jiang, Y., & Chen, Q. (2002). Effect of fluctuating wind direction on cross natural ventilation in buildings from large eddy simulation. *Building and Environment*, 37, 379–386.
- Jomehzadeh, F., Nejat, P., Calautit, J. K., Yusof, M. B. M., Zaki, S. A., Hughes, B. R., & Yazid, M. N. A. W. M. (2017). A review on windcatcher for passive cooling and natural ventilation in buildings, part 1: Indoor air quality and thermal comfort assessment. *Renewable and Sustainable Energy Reviews*, 70, 736–756.
- Kelly, M. (2009). Retrofitting the existing UK building stock. *Building Research & Information*, 37, 196–200. doi:10.1080/09613210802645924
- Khan, N., Su, Y., & Riffat, S. B. (2008). A review on wind driven ventilation techniques. *Energy and Buildings*, 40, 1586–1604.
- King, M. F., Gough, H. I., Halios, C., Barlow, J. F., Roberston, A., Hoxey, R., & Noakes, C. J. (2017). Investigating the influence of neighbouring structures on natural ventilation potential of a full-scale cubical building using time-dependent CFD. *Journal of Wind Engineering and Industrial Aerodynamics*, 169, 265–279.
- Kirimtat, A., Koyunbaba, B. K., Chatzikonstantinou, I., & Sarayildiz, S. (2016). Review of simulation modeling for shading devices in buildings. *Renewable and Sustainable Energy Reviews*, 53, 23–49.
- Li, B., & Yao, R. (2012). Building energy efficiency for sustainable development in China: Challenges and opportunities. *Building Research & Information*, 40, 417–431.
- Li, B., Yao, R., Wang, Q., & Pan, Y. (2014). An introduction to the Chinese evaluation standard for the indoor thermal environment. *Energy and Buildings*, 82, 27–36.
- Li, B., Yu, W., Liu, M., & Li, N. (2011). Climatic strategies of indoor thermal environment for residential buildings in Yangtze river region, China. *Indoor and Built Environment*, 20, 101–111.
- Li, L., & Mak, C. M. (2007). The assessment of the performance of a windcatcher system using computational fluid dynamics. *Building and Environment*, 42, 1135–1141.
- Liu, M. (2017). Usage characteristics of room air conditioner RAC in Chongqing area based on big data monitoring. *8th International Conference on Sustainable Development in Building and Environment (SuDBE) Conference*.
- Liu, Y., Liu, T., Ye, S., & Liu, Y. (2018). Cost-benefit analysis for energy efficiency retrofit of existing buildings: A case study in China. *Journal of Cleaner Production*, 177, 493–506.
- Lomas, K. J. (2007). Architectural design of an advanced naturally ventilated building form. *Energy and Buildings*, 39, 166–181.
- Lomas K. J., Giridharan R., Short C. A., & Fair A. J. (2012). Resilience of 'Nightingale' hospital wards in a changing climate. *Building Services Engineering Research and Technology*, 33, 81–103.
- Luo, J., & Gale, A. (2000). The evolution of the Chinese construction industry. *Building Research & Information*, 28, 51–58.
- Mak, C. M., Niu, J. L., Lee, C. T., & Chan, K. F. (2007). A numerical simulation of wing walls using computational fluid dynamics. *Energy and Buildings*, 39, 995–1002.
- Mandalaki, M., Zervas, K., Tsoutsos, T., & Vazakas, A. (2012). Assessment of fixed shading devices with integrated PV for efficient energy use. *Solar Energy*, 86, 2561–2575.
- Meroney, R. N. (2009). CFD prediction of airflow in buildings for natural ventilation. *11th Americas Conference on Wind Engineering*.
- Ministry of Housing Urban and Rural Development (MOHURD), National Development and Reform Commission (NDRC). (2013). Green building action plan, Ministry of Housing and Urban-Rural Development of the People's Republic of China and National Development and Reform Commission.
- Mochida, A., Yoshino, H., Takeda, T., Kakegawa, T., & Miyauchi, S. (2005). Methods for controlling airflow in and around a building under cross-ventilation to improve indoor thermal comfort. *Journal of Wind Engineering and Industrial Aerodynamics*, 93, 437–449.

- Montazeri, H. (2011). Experimental and numerical study on natural ventilation performance of various multi-opening wind catchers. *Building and Environment*, 46, 370–378.
- Montazeri, H., & Montazeri, F. (2018). CFD simulation of cross-ventilation in buildings using rooftop wind-catchers: Impact of outlet openings. *Renewable Energy*, 118, 502–520.
- Muhsin, F., Yusoff, W. F. M., Mohamed, M. F., & Sapian, A. R. (2017). CFD modeling of natural ventilation in a void connected to the living unit of multi-storey housing for thermal comfort. *Energy and Buildings*, 144, 1–16.
- National Development and Reform Commission (NDRC). (2011). *Medium and long term development plan for renewable energy in China*. Beijing: Author. [in Chinese]
- Nejat, P., Calautit, J. K., Majid, M. Z. A., Hughes, B. R., Zeynali, I., & Jomehzadeh, F. (2016). Evaluation of a two-sided windcatcher integrated with wing wall (as a new design) and comparison with a conventional windcatcher. *Energy and Buildings*, 126, 287–300.
- Omraní, S., García-Hansen, V., Capra, B., & Drogemuller, R. (2017). Natural ventilation in multi-storey buildings: design process and review of evaluation tools. *Building and Environment*, 116, 182–194.
- Pain, C., Umpleby, A., De Oliveira, C., & Goddard, A. (2001). Tetrahedral mesh optimisation and adaptivity for steady-state and transient finite element calculations. *Computer Methods in Applied Mechanics and Engineering*, 190, 3771–3796.
- Pavlidis, D. (2011). *Modelling urban air quality using mesh adaptive large-eddy simulation* (PhD thesis). Imperial College London.
- Pavlidis, D., Gorman, G., Gomes, J., Pain, C., & ApSimon, H. (2010). Synthetic-eddy method for urban atmospheric flow modelling. *Boundary-Layer Meteorology*, 136, 285–299.
- Peren, J. I., Van Hooff, T., Leite, B. C. C., & Blocken, B. (2015a). CFD analysis of cross-ventilation of a generic isolated building with asymmetric opening positions: Impact of roof angle and opening location. *Building and Environment*, 85, 263–276.
- Peren, J. I., Van Hooff, T., Leite, B. C. C., & Blocken, B. (2015b). Impact of eaves on cross-ventilation of a generic isolated leeward sawtooth roof building: Windward eaves, leeward eaves and eaves inclination. *Building and Environment*, 92, 578–590.
- Peren, J. I., Van Hooff, T., Leite, B. C. C., & Blocken, B. (2016). CFD simulation of wind-driven upward cross ventilation and its enhancement in long buildings: Impact of single-span versus double-span leeward sawtooth roof and opening ratio. *Building and Environment*, 96, 142–156.
- Prajongsan, P., & Sharples, S. (2012). Enhancing natural ventilation, thermal comfort and energy savings in high-rise residential buildings in Bangkok through the use of ventilation shafts. *Building and Environment*, 50, 104–113.
- Priyadarsini, R., Cheong, K. W., & Wong, N. H. (2004). Enhancement of natural ventilation in high-rise residential buildings using stack system. *Energy and Buildings*, 36, 61–71.
- Ramponi, R., & Blocken, B. (2012). CFD simulation of cross-ventilation for a generic isolated building: Impact of computational parameters. *Building and Environment*, 53, 34–48.
- Ramponi, R., Blocken, B., De Coo, L. B., & Janssen, W. D. (2015). CFD simulation of outdoor ventilation of generic urban configurations with different urban densities and equal and unequal street widths. *Building and Environment*, 92, 152–166.
- Saadatian, O., Chin, L., Sopian, H. K., & Sulaiman, M. Y. (2012). Review of windcatcher technologies. *Renewable and Sustainable Energy Reviews*, 16, 1477–1495.
- Salim, S. M., Ong, K. C., & Cheah, S. C. (2011). Comparison of RANS, URANS and LES in the prediction of airflow and pollutant dispersion. *Proceedings of the World Congress on Engineering and Computer Science*.
- Schulze, T., & Eicker, U. (2013). Controlled natural ventilation for energy efficient buildings. *Energy and Buildings*, 56, 221–232.
- Short, C. A. (2017). *The recovery of natural environments in architecture*. Abingdon: Taylor and Francis, Routledge. Chapter 9.
- Short, C. A., Cook, M., Cropper, P. C., & Al-Maiyah, S. (2010). Low energy refurbishment strategies for health buildings. *Journal of Building Performance Simulation*, 3, 197–216.
- Short, C. A., Cook, M., & Lomas, K. J. (2009). Delivery and performance of a low-energy ventilation and cooling strategy. *Building Research & Information*, 37(1), 1–30. doi:10.1080/09613210802607841
- Short, C. A., Lomas, K. J., Giridharan, R., & Fair, A. J. (2012). Building resilience to overheating into 1960s UK hospital buildings within the constraint of the national carbon reduction target: Adaptive strategies. *Building and Environment*, 55, 73–95.
- Short, C. A., Lomas, K. J., & Woods, A. (2004). Design strategy for low energy ventilation and cooling within an urban heat island. *Building Research & Information*, 32(3), 187–206 doi:10.1080/09613210410001679875
- Short, C. A., Noakes, C. J., Gilkeson, C. A., & Fair, A. (2014). Functional recovery of a resilient hospital type. *Building Research & Information*, 42(6), 657–684. doi:10.1080/09613218.2014.926605
- Short, C. A., Renganathan, G., & Lomas, K. J. (2015). A medium-rise 1970s maternity hospital in the east of England: Resilience and adaptation to climate change. *Building Services Engineering Research and Technology*, 36, 247–274.
- Short, C. A., Yao, R., Luo, G., & Li, B. (2012). Exploiting a hybrid environmental design strategy in the continental climate of Beijing. *International Journal of Ventilation*, 11, 105–130.
- Song, J. (2017). A preliminary report on indoor thermal comfort evaluation for naturally ventilated building environment over hot summer & cold winter region in China. *LoHCool Project Working Paper*, unpublished.
- Song, J., Fan, S., Lin, W., Mottet, L., Woodward, H., Davies Wykes, M., Arcucci, R., Xiao, D., Debay, J., ApSimon, H., Aristodemou, E., Birch, D., Carapentieri, M., Fang, F., Herzog, M., Hunt, G.R., Jones, R.L., Pain, C., Pavlidis, D., Robins, A.G., Short, C.A., & Linden, P. (2018). Natural ventilation in cities: The implications of fluid mechanics. *Building Research & Information*, 46(8). doi:10.1080/09613218.2018.1468158
- Su, H., Riffat, S. B., Lin, Y.-L., & Khan, N. (2008). Experimental and CFD study of ventilation flow rate of a Monodraught™ windcatcher. *Energy and Buildings*, 40, 1110–1116.
- Swiegers, J. J. (2015). *Inlet and outlet shape design of natural circulation building ventilation systems* (Master's thesis). Faculty of Engineering at Stellenbosch University.

- Tong, Z., Chen, Y., & Malkawi, A. (2016). Defining the influence region in neighborhood-scale CFD simulations for natural ventilation design. *Applied Energy*, 182, 625–633.
- Tong, Z., Chen, Y., Malkawi, A., Adamkiewicz, G., & Spengler, J. D. (2016). Quantifying the impact of traffic-related air pollution on the indoor air quality of a naturally ventilated building. *Environment International*, 89–90, 138–146.
- Tong, Z., Chen, Y., Malkawi, A., Liu, Z., & Freeman, R. B. (2016). Energy saving potential of natural ventilation in China: The impact of ambient air pollution. *Applied Energy*, 179, 660–668.
- Tsinghua University Building Energy Research Centre (THUBERC). (2015). *2015 annual report on China building energy efficiency*. Beijing: China Construction Industry Publ.
- Van Hooff, T., & Blocken, B. (2010). Coupled urban wind flow and indoor natural ventilation modelling on a high-resolution grid: A case study for the Amsterdam Arena stadium. *Environmental Modelling and Software*, 25, 51–65.
- Van Hooff, T., Blocken, B., Aanen, L., & Bronsema, B. (2011). A Venturi-shaped roof for wind-induced natural ventilation of buildings: Wind tunnel and CFD evaluation of different design configurations. *Building and Environment*, 46, 1797–1807.
- Van Hooff, T., Blocken, B., Aanen, L., & Bronsema, B. (2012). Numerical analysis of the performance of a Venturi-shaped roof for natural ventilation: Influence of building width. *Journal of Wind Engineering and Industrial Aerodynamics*, 104–106, 419–427.
- Van Hooff, T., Blocken, B., & Tominaga, Y. (2017). On the accuracy of CFD simulations of cross-ventilation flows for a generic isolated building: Comparison of RANS, LES and experiments. *Building and Environment*, 114, 148–165.
- Wang, L., & Wong, N. H. (2008). Coupled simulations for naturally ventilated residential buildings. *Automation in Construction*, 17, 386–398.
- Wang, S. S., Zhou, D. Q., Zhou, P., & Wang, Q. W. (2011). CO₂ emissions, energy consumption and economic growth in China: A panel data analysis. *Energy Policy*, 39, 4870–4875.
- Wu, W., Zhai, J., Zhang, G., & Nielsen, P. V. (2012). Evaluation of methods for determining air exchange rate in a naturally ventilated dairy cattle building with large openings using computational fluid dynamics (CFD). *Atmospheric Environment*, 63, 179–188.
- Wu, Y. C., Yang, A. S., Tseng, L. Y., & Liu, C. L. (2011). Myth of ecological architecture designs: Comparison between design concept and computational analysis results of natural-ventilation for Tjibaou cultural center in New Caledonia. *Energy and Buildings*, 43, 2788–2797.
- Yang, A. S., Wen, C. Y., Juan, Y. H., Su, Y. M., & Wu, J. H. (2014). Using the central ventilation shaft design within public buildings for natural aeration enhancement. *Applied Thermal Engineering*, 70, 219–230.
- Yao, R., Li, B., & Liu, J. (2009). A theoretical adaptive model of thermal comfort – adaptive predicted mean vote (aPMV). *Building and Environment*, 44, 2089–2096.
- Yusoff, W. F. M., Salled, E., Adam, N. M., Sapian, A. R., & Sulaiman, M. Y. (2010). Enhancement of stack ventilation in hot and humid climate using a combination of roof solar collector and vertical stack. *Building and Environment*, 45, 2296–2308.
- Zha, X., Zhang, J., & Qin, M. (2017). Experimental and numerical studies of solar chimney for ventilation in low energy buildings. *10th International Symposium on Heating, Ventilation and Air Conditioning, ISHVAC2017, Procedia Engineering* (205, pp. 1612–1619).
- Zhang, X. P., & Cheng, X. M. (2009). Energy consumption, carbon emissions, and economic growth in china. *Ecological Economics*, 68, 2706–2712.
- Zhang, Y., He, C. O., Tang, B. J., & Wei, Y. M. (2015). China on emissions and economic in China. *Energy and Buildings*, 94, 240–251.
- Zhejiang Climate Center. (2017). Zhejiang climate impact assessment report for summer 2017. Retrieved from <http://zj.weather.com.cn/qhbh/index.shtml>
- Zhou, C., Wang, Z., Chen, Q., Jiang, Y., & Pei, J. (2014). Design optimization and field demonstration of natural ventilation for high-rise residential buildings. *Energy and Buildings*, 82, 457–465.